Contrast enhancement with the noise removal by a discriminative filtering process

Badrun Nahar

A Thesis

in

The Department

of

Electrical and Computer Engineering

Presented in Partial Fulfillment of the Requirements

for the Degree of Master of Applied Science (Electrical and Computer Engineering) at

Concordia University

Montreal, Quebec, Canada

August, 2012

CONCORDIA UNIVERSITY
SCHOOL OF GRADUATE STUDIES

This is to certify that the thesis prepared

By: Bardun Nahar

Entitled: "Contrast enhancement with the noise removal by a discriminative filtering process"

and submitted in partial fulfillment of the requirements for the degree of

Master of Applied Science

Complies with the regulations of this University and meets the accepted standards with respect to originality and quality.

Signed by the final examining committee:

_____ Chair
Dr. R. Raut

_____ Examiner, External
Dr. Y. Zeng (CIISE) To the Program

_____ Examiner
Dr. W-P. Zhu

_____ Supervisor
Dr. C. Wang

Approved by: _____
Dr. W. E. Lynch, Chair
Department of Electrical and Computer Engineering

_____20_____ _____
Dr. Robin A. L. Drew
Dean, Faculty of Engineering and
Computer Science

Abstract

Contrast enhancement with the noise removal by a discriminative filtering process

Badrun Nahar

In many image processing tasks, a good contrast is essential for a better interpretability and extraction of image features. Hence, a contrast enhancement is necessary if the image to be processed has a poor quality. Numerous methods of contrast enhancement have been developed based on various data transformations. However, in the application of any of the existing method, one has to handle the problem of the conflict of the degree of enhancement and noise created in the process, and/or that of a good quality of the enhancement versus the cost of computation.

In this thesis, a method of contrast enhancement is proposed. It combines a histogram equalization to enhance the gray-level gradients and a low-pass filtering to remove the noise created by the inappropriate enhancement in some regions of the image. Such regions need to be identified for an effective noise removal without losing signal gray level variations. The emphasis in the development of the filtering process is to make the low-pass operations discriminative according to the presence of noises and signal variations in different regions for a good signal preservation. Also, as the noise and signal often co-exist in a region, the balance between the preservation of signal gradients and the removal of the assumed noise variations is different from region to region. The low-pass filtering applied to the regions having some signal

edges should not be the same as that to very flat ones. In the proposed method, a low-pass filtering of different smoothing is implemented by successive stages of simple low-pass filters. It is applied to different regions by means of different masks controlling the operations in the stages. A classification process is designed to identify the pixels in different regions, and based on the classification results, the controlling masks are generated. The classification and the mask generation are implemented by using very simple logic operations. The overall complexity of the proposed enhancement is very low, compared with those reported. The simulation results demonstrated that the proposed method lead to a superior quality of the contrast enhancement of varieties of images, in terms of visual quality and measurement of preservation of edges.

Acknowledgement

At first, I would like to express my sincere gratitude to my supervisor Dr. Chunyan Wang for her immense support and brilliant guidance throughout my tenure in this thesis work. Her knowledge and expertise in the field enriches me a lot and opens new doors of thoughts and understanding to me. I feel extremely privileged to be able to work under her supervision.

And also I thank my family and friends who were always beside me with their love, affection and valuable suggestions.

Finally, all praises and thanks to my Creator Who gave me the strength to successfully finish this thesis work.

Table of Contents

List of Figures

List of Tables

List of Acronyms and Abbreviations

HE	Histogram Equalization
CLAHE	Contrast Limited Adaptive Histogram Equalization
LP	Low-Pass
PDF	Probability Density Function
BMM	Bidirectional Multi-stage Median
PFOM	Pratt's Figure of Merit
PSNR	Peak Signal to Noise Ratio

List of Symbols

I	Input image
I_C	Contrast enhanced image
I_G	Pre-filtered image by Gaussian
I_{bw}'	Binary mask generated by coarse classification process by thresholding
I_{bw}	Binary mask generated after fine-tuning by the region correction process
I_o	Output image
σ	Standard deviation of Gaussian filter
G	Gray level
G_{peak}	Gray level at the peak of the histogram
$n_p(G)$	Number of pixels at gray level G
n_{total}	Total number of the pixels classified as in the homogeneous regions
n_{miss}	Number of pixels from non-homogeneous regions misclassified as in homogeneous regions
$\frac{n_{miss}}{n_{total}}$	Misclassification rate of pixels belonging to homogeneous regions

List of Terminology

Homogeneous pixels	The pixels which truly belong to homogeneous regions.
Non-homogeneous pixels	The pixels which truly belong to non-homogeneous regions.

Chapter 1

Introduction

Many research themes in digital image processing are about the improvement of image quality. Enhancing the contrast to reveal sufficient details of objects and background in an image is often required in various image processing tasks. Images of poor contrast are often produced due to various reasons and thus a contrast enhancement become necessary before being processed for a particular purpose. The quality of the enhancement will affect the quality of the processes in the succeeding stages.

There are varieties of contrast enhancement methods. Each has its advantages and drawbacks. In this chapter, the background of this study and its importance are described. The motivations and the objective of the work are stated. Also the scope of the work and the organization of the thesis are presented.

1.1 Contrast enhancement and the challenges

Low contrast images are often produced under poor conditions of image acquisition. For example, if a natural scene of rich intensity variation, often referred to as high dynamic scene, is acquired by a camera of standard dynamic range that is much narrower than that of the scene, the original image will have regions under-exposed and over-exposed, resulting in a poor contrast. In case of medical imaging, the projection has to be low-dosed to reduce the damage to the body

tissues, and the projected image may have a very low contrast. In some other cases, the image contrast may be reduced by transmission.

The problem of poor contrast is reflected as poor gradients, representing signal attenuations in an image. It affects the results of the image processing in many aspects. In particular, it makes the edge detection more difficult, which may lead to a severe degradation to the overall processing quality.

There are various approaches to a contrast enhancement. Some are done in the process of image acquisition by high dynamic imaging (HDI). It is to use a multi-exposure technique to acquire multiple images of the same scene and to merge those together [5]. Others are to enhance the gray level variations in the acquired images. Varieties of data transform are used for this purpose and the most commonly used is the histogram equalization (HE). It is to remap gray levels based on probability density function of an image so that the gray level distribution of the image becomes more even as shown in Figure 1.1. However, no matter which transform method is used for a contrast enhancement, there are always concerns of noise introduced in the process. In general, the degree of the contrast enhancement seems to contradict the noise level of the enhanced image. On one hand, advanced histogram equalization methods are developed to target the problem of enhancement-noise conflict. More sophisticated forms of the pixel mapping functions may help to reduce the severity of the problem, usually at the expense of more complex computation [21] [29]. On the other hand, filtering process can be added to reduce the noise [23] [4] [15]. However, a simple filtering can also erase enhanced signal variations whereas a sophisticated filtering may also require a large amount of computation. Developing contrast enhancement methods that are effective for the improvement of the contrast, and reduction of the noise and computation cost is a challenging task.

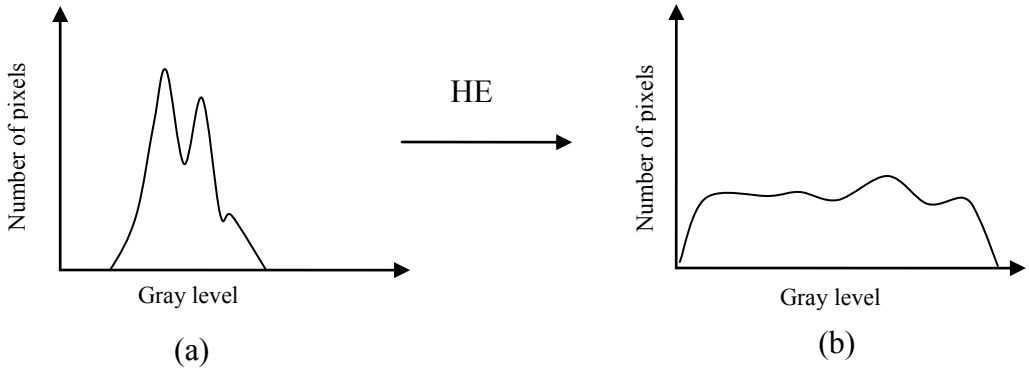

Figure 1.1 (a) Histogram of a low-contrast image.
(b) Histogram after the HE process

1.2 Motivations and objective

A good image contrast facilitates the task of further processes in image processing such as feature extractions. Developing an effective method of image contrast enhancement, in terms of computation efficiency, is important for the design of algorithms that lead to an easy implementation.

The objective of the work presented in the thesis is to develop a computation-efficient method for image contrast enhancement. The emphasis of the work is on the minimization of the noise produced in the process of the enhancement. It aims at a good image contrast with the best preservation of gray level variations of image signal.

1.3 Scope and organization of this thesis

To achieve the above-mentioned objective, the work will be in the topic areas of histogram equalization for the contrast enhancement, and the filtering operations to remove the noise

created in the HE process. The main task is to develop a low-pass filtering method to remove the noise without erasing the signal variations in the image. Hence, the filtering process will involve a pixel classification so that the smoothing operations performed by the low-pass filters will be effectively discriminative in the image space.

The thesis is organized as follows. In chapter 2, the basics about the contrast enhancement and low-pass filtering are described. Some of the existing work relevant to this one is also presented. The description of the proposed enhancement method is presented in chapter 3. In particular, the approach to the discriminative filtering and the pixel classification is described in an elaborate manner. A performance evaluation of the image enhancement process developed with the proposed method is found in chapter 4. The subjective observations of the simulation results and the objective measurements are presented. The work of the thesis and results are summarized in chapter 5.

Chapter 2

Background and the relevant work in the topic domain

Images of good contrast are essential in different image processing tasks. But acquiring a good contrast image directly from the acquisition device is not always possible because of the limitation of those devices and the improper illumination conditions of surroundings. Hence, the enhancement of image contrast is an important pre-process in many application areas of image processing. Contrast of an image can be improved by increasing the gray level shades among the objects and background of an image. By means of different data transformation method, e.g., histogram equalization, wavelet transform etc., image contrast can be enhanced. Since, HE method is one of the simplest and effective method, HE-based contrast enhancement is employed in many applications. However, some undesired gray level variations are introduced in the image during the enhancement by the HE process, those degrade the image quality. So, it is important to employ some procedure in the HE process that can erase these variations.

Several approaches are found in the literature those are developed to reduce these undesired gray level variations, i.e., noises. Some of these approaches [1] [21] are based on the modulation of the parameters involved in the mapping function according to some homogeneity criteria. These kinds of modulated functions sometimes are not able to enhance the contrast sufficiently in some specific regions in order to suppress the visibility of noise. Some mapping functions of such kind provide good enhancement, but are controlled by sophisticated modulation of parameters that make the overall procedure highly computation intensive. Besides these

approaches, there are some other approaches [23] [4] [15] those employ low-pass operation after the contrast enhancement process. The low-pass operation in this case needs to be discriminative so that it can distinguish different regions of the image and adjust the degree of smoothing depending on the severity of noises and presence of signal variations in different regions. This discriminativeness is to ensure the effective removal of noise without affecting the signal variations. The challenge of this kind of approach is to design an appropriate procedure for classifying the image regions and choosing proper low-pass filters that suit the image application in terms of noise removal, preservation of fine details and computation efficiency.

In this chapter, some background knowledge of HE-based contrast enhancement methods, low-pass filters and classification procedures will be presented in the sub-sections 2.1.1, 2.1.2 and 2.1.3, respectively. In § 2.2, some existing works relevant to this thesis will be introduced.

2.1 Basics of image processing related to the proposed method

As the method of contrast enhancement developed in this work involves HE-based contrast enhancement followed by discriminative low-pass operation, it is necessary to study the existing works related to each process of this method. Hence, in the following sub-sections, the state of the art methods of the HE-based contrast enhancement, the low-pass filtering and classification procedures are included.

2.1.1 Histogram equalization for image contrast enhancement

Histogram equalization is being used in different application areas of image processing for contrast enhancement due to its simplicity and effectiveness. Standard HE process enhances the global contrast of an image by distributing the pixels of the entire image uniformly among all the gray levels. The normalized histogram of the image is approximated as its probability density function (PDF). Based on this PDF, a non-linear mapping function is generated that maps the new gray level values for each of the old gray level. The mapping function $T(r)$ of the HE process [Gonzalez & Woods, 2002] can be expressed as,

$$s_k = T(r_k) = \sum_{j=0}^{k} p_r(r_j) = \sum_{j=0}^{k} \frac{n_j}{n}, \qquad k = 0, 1, \ldots, L-1.$$

Here, s_k is the new gray level value for the input gray level r_k, $p_r(r_j)$ is the PDF of the input gray level j, n is the total number of pixels in the input image and n_j is the number of pixels having gray level j . In Figure 2.1, the mapping function of the HE process is illustrated.

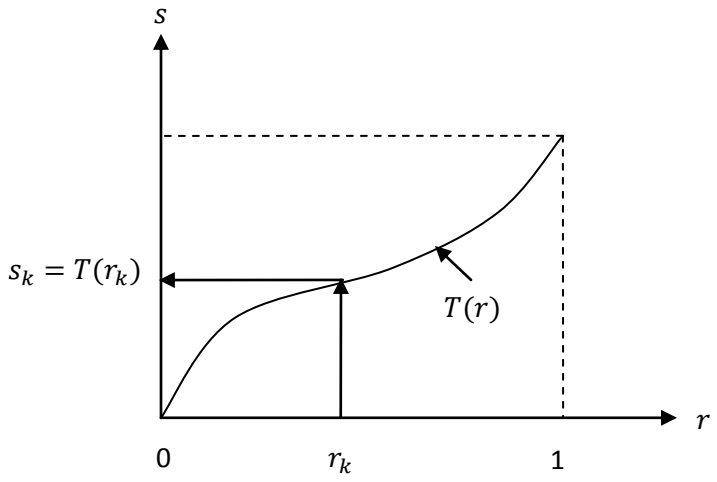

Figure 2.1 Gray level mapping function in the HE process [8].

HE process is effective when the background and objects both are dark or bright. But the contrast of the images with both under-exposed and over-exposed regions cannot be enhanced effectively by it. Moreover, it creates some undesirable effects like over-enhancement of more-frequent gray levels and loss of contrast for less-frequent gray levels. To overcome the shortcomings of the standard HE method, many improved HE-based methods have been developed and proposed. The proposed methods, generally, belong to two types: the adaptive (local) HE methods (AHE) [14] [25] [6], and the improved global methods [27] [28] based on normal HE.

AHE methods are able to enhance the local contrast and thereby reveal more details. Basic AHE computes the HE mapping for each pixel based on a contextual region surrounding the pixel. This method brings out more detail than HE. However, it over-amplifies noises in homogeneous regions and it is computationally very intensive. Later many variants of AHE have been developed to address the problems of the basic AHE. Contrast Limited Adaptive Histogram Equalization (CLAHE) is one of such variants, which has controllable parameter to limit the contrast. In CLAHE process, the input image is divided into a number of tiles. Optimal number of tiles depends on the type of input image. For each tile, the histogram of the contained pixels is calculated. Based on a desired limit for contrast enhancement, a clip limit is decided for clipping the histogram. The higher the clip limit, the more the contrast enhancement. This clip limit fixes the maximum number of pixels allowed in each histogram bin. The pixels that exceed this clip limit are redistributed equally in all the histogram bins until they do not go below the clip limit. The obtained histogram is then normalized and used to estimate the new gray levels using the HE mapping function. These new mapping functions result artificially induced boundary among the neighbouring tiles. To eliminate this boundary effects, bilinear interpolation is performed.

The CLAHE algorithm was originally developed for medical imaging and has proven to be successful for the enhancement of low-contrast images too. However, it has some drawbacks. If the contrast is increased, noise also increases specially in homogeneous regions. A low-pass filtering operation after the CLAHE process can be employed to smooth the noise and improve the overall quality of the enhancement.

2.1.2 Low-pass filters

In digital image processing, to remove the undesired gray level variations, i.e., noises from an image, low-pass filtering is generally employed. Numbers of low-pass filters have been developed for de-noising, such as simple Gaussian filters [8], Yaroslavsky neighborhood filters [9], bilateral filters [26], non-local mean filters [20], anisotropic diffusion filters [22], median-based filters [10], and so on. Each filter has its own merits and demerits depending on the priority of the application. Some filters are more efficient to remove the noise while blurring the image, whereas some are capable of moderate noise removal with good preservation of signal variations. Also, the computational complexity of each filter is different.

Gaussian filter is one of the simplest low-pass filters used for noise removal. It effectively eliminates the high-frequency noises, but blurs the fine details and sharp edges of the image. It smoothes the image by replacing the center pixel with the weighted average of the neighboring pixels. The weights are calculated from the Gaussian function, $(x, y) = \frac{1}{2\pi\sigma^2} e^{-\frac{x^2+y^2}{2\sigma^2}}$, where σ is the standard deviation. The higher the σ value, the higher the degree of noise removal and blurring.

Yaroslavsky filter is a de-noising filter based on non-local algorithm. It takes a weighted average of the values of the pixels which are from a particular neighborhood. The neighborhood consists of the pixels which are both close in terms of gray level values and spatial distance to the center pixel. If the neighborhood based on gray level proximity and spatial distance proximity are defined by $B(i,h)$ and $B_\rho(i)$, respectively, where

$B(i,h) = \{ j \in I \mid u(i) - h < u(i) < u(i) + h \}$ with u being the original image, I being the gray level value and $B_\rho(i)$ is a ball of center i and radius ρ, the total neighborhood of the Yaroslavsky filter is $B(i,h) \cap B_\rho(i)$. The closed form of the filter is expressed as,

$$Y_u(\boldsymbol{x}) = \frac{1}{C(\boldsymbol{x})} \int_{B_\rho(\boldsymbol{x})} u(\boldsymbol{y})\ e^{-\frac{|u(\boldsymbol{y})-u(\boldsymbol{x})|^2}{\sigma^2}}\ d\boldsymbol{y}$$

where, $C(\boldsymbol{x}) = \int_{B_\rho(\boldsymbol{x})} e^{-\frac{|u(\boldsymbol{y})-u(\boldsymbol{x})|^2}{\sigma^2}}\ d\boldsymbol{y}$ is the normalization factor, $u(\boldsymbol{x})$ and $u(\boldsymbol{y})$ are the gray level of the center pixel and the neighborhood pixel, respectively, and σ is the degree of filtering.

A more sophisticated variant of Yaroslavsky filter is the bilateral filter. It is expressed as,

$$h(\boldsymbol{x}) = \frac{1}{C(\boldsymbol{x})} \int_{B_\rho(\boldsymbol{x})} w(\boldsymbol{x},\boldsymbol{y})\ \emptyset\big(u(\boldsymbol{x}),u(\boldsymbol{y})\big)u(\boldsymbol{y})\ d\boldsymbol{y}$$

where, $C(\boldsymbol{x}) = \int_{B_\rho(\boldsymbol{x})} w(\boldsymbol{x},\boldsymbol{y})\ \emptyset\big(u(\boldsymbol{x}),u(\boldsymbol{y})\big)\ d\boldsymbol{y}$ is the normalization factor. The two weighting factors of this filter, $w(\boldsymbol{x},\boldsymbol{y}) = w(\boldsymbol{x}-\boldsymbol{y})$ and $\emptyset\big(u(\boldsymbol{x}),u(\boldsymbol{y})\big) = \emptyset\big(u(\boldsymbol{x})-u(\boldsymbol{y})\big)$. These are the weights corresponding to spatial distance and gray level proximity, respectively. This kind of filter usually performs better than Gaussian filters in terms of preservation of fine details while eliminating noise. But the computation complexity is much higher.

Median based filters are non-linear filters, which have a good quality of preservation of signal variations during noise smoothing, even if the signal variations and the noise occupy the same frequency band. Theses filters are based on order statistics. A basic square median filter arranges all the pixels of a small window in sequential order, and replaces the center pixel with the middle value of the ordered set. Since the replaced values consist one of those present in the neighborhood unlike the average filters, it is more efficient to preserve the signal variations. And also, as it does not introduce any unrealistic gray level values during the filtering process, it can be used repeatedly to strengthen the noise smoothing. However, there are some demerits of square median filters. It cannot preserve the corners of the image objects and also erases the thin lines. To overcome the problems of square median filters, many advanced median-based filters are developed, such as weighted median filters [19], median hybrid filters [13], multi-stage median filters [12] [17], and so on.

In multi-stage median filters, instead of one median operation, several stages of median filters are used. The main idea is to combine the outputs of some basic sub-filters where each of them is designed to preserve the signal variations in certain orientations. The bidirectional multi-stage median (BMM) filter is one of the variants of such filters. It takes the median value of a set consisting of the center pixel, the median of the diagonal pixels, and the median of the orthogonal pixels. The total procedure can be expressed as follows.

Let us consider a square window $\boldsymbol{W}$ of size $(2n+1) \times (2n+1)$. The diagonal pixels shown in Figure 2.2 (a) form the diagonal kernel $\boldsymbol{W_D}$, the orthogonal pixels in Figure 2.2(b) form the orthogonal kernel $\boldsymbol{W_O}$ and $x(i,j)$ is the center pixel. Then, the output of the BMM filter can

be expressed as,

$$y(i,j) = Median\{ Median(\boldsymbol{W_D}),\ Median(\boldsymbol{W_O}),\ x(i,j) \}.$$

Here, $\boldsymbol{W_D} = \boldsymbol{W_1} \cap \boldsymbol{W_2}$ such that $\boldsymbol{W_1} = \{ x(i+k, j+k), -n \le k \le n,\ k \ne 0 \}$,

$$\boldsymbol{W_2} = \{ x(i-k, j+k), -n \le k \le n, k \ne 0 \},$$

And $\boldsymbol{W_O} = \boldsymbol{W_3} \cap \boldsymbol{W_4}$ such that $\boldsymbol{W_3} = \{ x(i, j+k), -n \le k \le n,\ k \ne 0 \}$ and

$$\boldsymbol{W_4} = \{ x(i+k, j), -n \le k \le n, k \ne 0 \}.$$

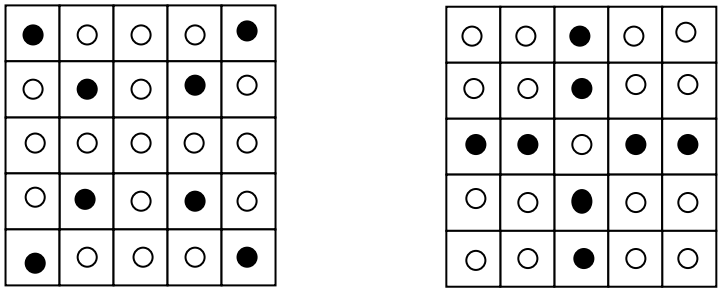

(a) (b)

Figure 2.2 (a) Diagonal kernel $\boldsymbol{W_D}$ formed by the black pixels.
(b) Orthogonal kernel $\boldsymbol{W_O}$ formed by the black pixels.

The performance of BMM filter is better than square median filters in terms of preservation of signal variations and implementation speed. It can be employed repeatedly in a low-pass filtering operation. Comparing to other sophisticated weighted average filter described earlier,

multi-stage median is computationally efficient and can better preserve the fine details while removing the noise.

2.1.3 Classification

Classification is a process that involves separating an image into regions having some measure of similarity among them. It is considered as an important basic operation for meaningful analysis and interpretation of an image. Classification approaches are largely application dependent. Researchers have extensively worked over this fundamental problem and proposed various methods based on region growing and shrinking methods, clustering methods and Boundary detection methods [7].

In the clustering method, image pixels are placed into several groups based on some measure of similarity within them. One of the standard clustering methods is thresholding of image histogram. Comparing to other types of methods, this method is the simplest. In this method, initially histogram of the entire image is calculated. Then, the shape of the histogram is analyzed and significant peaks are identified. The best peaks are selected and gray level thresholds are set on either side of each peak. The image is classified into regions based on these peaks. An illustration of this image thresholding is presented in Figure 2.3.

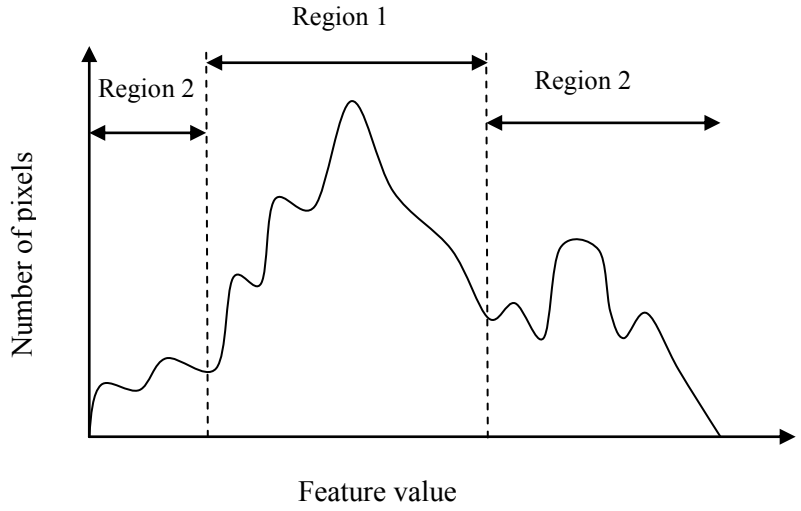

Figure 2.3 Classification of image by thresholding. Two thresholds are selected, one of each side of the peak. Then the image is divided into two regions. Region 1 corresponds to those pixels with feature values between the selected thresholds. Region 2 consists of those pixels with feature values outside the threshold [7].

This kind of classification is particularly very effective for low-contrast images as these images have significant peaks in their histograms. The accuracy of the classification largely depends on proper threshold selection. Many research works have been done to define an effective way of threshold selection [24].

After the thresholding of an image, there may remain some misclassified pixels. To minimize this misclassification, some region correction [18] algorithm can be employed. This kind of algorithm identifies the misclassified pixels by checking their similarity with their neighbors connected along different directions. If the neighbors having the similar status of a pixel form certain patterns, they can be considered as a misclassified pixel and their status will be corrected. Thus the region correction algorithm helps to increase the precision of

classification. Since, the thresholded image is usually a binary image and region correction is applied on it, the overall procedure is computationally efficient.

2.2 Relevant approaches related to the thesis work

The aim of the work in this thesis is effective removal of noise from a contrast enhanced image with preservation of signal variations. When the contrast of an image is enhanced by means of some enhancement process like HE-based methods, undesired gray level variations are introduced in the image. These undesired variations are mostly visible in homogeneous regions those degrade the overall image quality. These noises need to be smoothed discriminatively in order to attain an effective removal of noise as well as a good preservation of signal details. To handle this kind of problem, different approaches are proposed in the literature. In this section, the generalized ways of solving this problem will be discussed and two state of the art methods will be described briefly.

Generally, there are two different approaches found in the literature to produce low-noise contrast enhanced image. One approach is to modify the mapping function of the contrast enhancement process [1] [21] in such a way that the undesired variations, i.e., noises are remained suppressed during the contrast enhancement. In this case, degree of revealing the details is sometimes compromised with the noise reduction. Sometimes the modified mapping functions become very sophisticated in terms of computational complexity. The other approaches [23] [4] [15] are to smooth the contrast enhanced image by the low-pass operation. The kind of low-pass operation needs to be discriminative so that it can distinguish the signal variations and

the noises of the enhanced image, and implement the smoothing only in the noisy regions in order not to damage the signal variations.

The goal of the work in [23] is to develop a universal approach to remove different kinds of artifacts and noises created after contrast or color modification. The authors denoted the noises as spatial irregularities of mapping function of contrast or color modification. They proceeded to regularize this irregularity with the help of Yaroslavsky filter in the following manner:

Given u is the original image, $T(u)$ is the contrast modified image. Then the mapping function irregularity is defined as, $M(u) := T(u) - u$. To regularize $M(u)$, they developed the transportation regularization map (TMR) filter as,

$$TMR_u(T(u)) = Y_u(T(u)) + u - Y_u(u).$$

In this regularization process, $Y_u(T(u))$ is blurred due to low pass filtering. The image detail $(u - Y_u(u))$ is added with it to restore the fine details. To make this regularization process iterative in order to removing artifacts effectively, the filtering process is organized as follows:

$$TMR_u^k\left(T(u)\right) = Y_u^k\left(T(u) - u\right) + u\,.$$

Here, Y_u^k refers to the recursive use of Y_u filter.

To decide the number of iterations, they compute a convergence map $C(x)$ as,

$$C(x) = ||Y_u^k\left(T(u) - u\right) - Y_u^{k-1}\left(T(u) - u\right)||$$

Iteration continues on a pixel x until the condition $C(x) > t$ is achieved. Here, t is the user defined threshold. When $C(x)$ becomes smaller than t, the iteration stops for that pixel. The whole procedure of the iterated TMR filtering is illustrated in Figure 2.4.

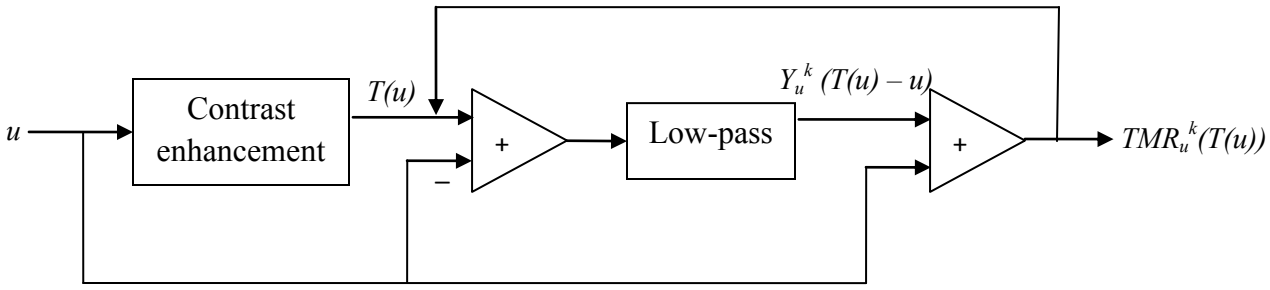

Figure 2.4 Iterated TMR filtering of contrast enhanced image [23]

The output quality produced by the iterated TMR filtering is actually depended on the quality of the input image since the original input is added with the low-pass filtered image in each iteration. So, its performance, in terms of contrast enhancement, degrades when the input image is a very low-contrast image. In terms of noise removal, though it performs well, but it erases the fine details like fine textures of image. The overall computational complexity of this process is heavy.

The work in [4] also aims at removing the noises from a contrast enhanced image. It does so by employing the projection onto convex sets (POCs) based post-processing after HE-based enhancement. In the post-processing, a convex set is computed that denotes possible range of output gray levels for a particular input gray level. Computation of the ranges is based on the mapping of the HE process. Using the convex set constraint, two sub-processes are carried out. First the HE-enhanced image is passed through a low-pass filter and after this process, the gray levels which move outside the range of convex set, they are revalued to the upper or lower boundary of the range. This sub-process is named as boundary condition. To suppress false

contour, dithering is applied at the end by adding a pseudorandom noise. The low-pass, boundary and dithering conditions are iteratively applied until the difference between two successive iterations becomes negligible. The overall procedure of this method is illustrated in Figure 2.4. This method is computationally intensive as the number of iterations required to effectively remove noises is high.

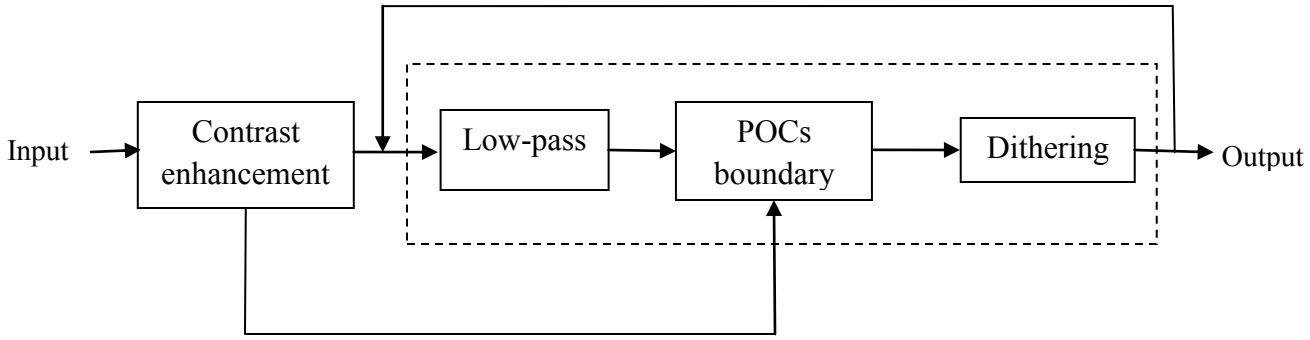

Figure 2.5 Enhancement of contrast followed by noise removal based on POCs post-processing [4].

2.3 Summary

Developing an effective method of noise removal from a contrast enhanced image is the main objective of this thesis work where emphasis is given to yield good preservation of signal variations and an efficient computation. The background of the processes those are involved in developing this proposed method is discussed in this chapter. In the beginning sub-sections of this chapter, state of the art methods related to each process are presented. Along with the procedural steps of the processes, their performances are mentioned briefly. In the later section,

some relevant works related to the proposed method are mentioned. The procedure and performance of two of those methods are described.

In the next chapter, detail of the proposed method will be presented. The design issues and challenges in developing each process involving the method will be discussed. Design of the two important procedures related to the proposed discriminative filtering, classification and low-pass filtering, will be described elaborately.

Chapter 3

Contrast enhancement with the noise removal by a discriminative filtering process

As described in Chapter 2, varieties of HE are used for contrast enhancement in image processing. However, an HE-based contrast enhancement often results in noises and artifacts which degrade the overall image quality. The objective of the work presented in this thesis is to enhance the image contrast with an effective removal of the noises and artifacts. The emphasis of the work is on the low-pass filtering with a good preservation of signal variations.

In an HE-based process, the gray level distribution of the original image is modified by using a non-linear mapping function, which creates, in many cases, some undesired gray level variations in the enhanced image, mostly appearing in homogeneous regions. Applying uniformly a straight-forward low-pass filtering leads to the loss of image details while removing those variations. It needs to design a discriminative low-pass filtering process to apply an appropriate dose of low-pass operation on selected noisy regions while the other regions with signal variations remain untouched. Such a discriminative filtering operation can be resource-demanding as the computation for the classification of the regions can be complex. The work presented in this thesis aims at developing a computation-efficient discriminative low-pass filtering process. In this process, the areas in the image space are discriminated, i.e. some are to be filtered and others are not. In the regions to be filtered, different low-pass filtering operations

are applied to different parts, depending on the severity of noises and also the priority of the preservation of signal variation in different regions.

The chapter is organized as follows. The first section presents an overview of the proposed method of contrast enhancement involving the low-pass process. The selection of the HE process for the contrast enhancement is described in § 3.2. The pre-filtering after the HE is discussed in § 3.3. Section 3.4 is dedicated to the detail description of the development of the pixel classification method and the creation of the masks. The design of the low-pass filters is presented in § 3.5.

3.1 Overview of the proposed method

The general scheme of HE-based contrast enhancement with noise reduction is shown in Figure 3.1. The low-pass filtering is often used to remove the noise and artifacts created in the HE. The challenging issue of the work in the contrast enhancement is to make the filtering discriminative to noise and signal variations.

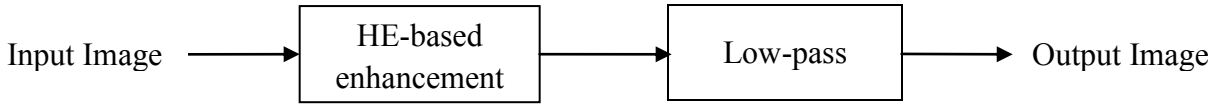

Figure 3.1 Block diagram of contrast enhancement involving noise reduction by LP filtering.

As mentioned previously, the noise and artifacts generated in the process of the HE are more visible in homogeneous regions. It is also to say that in less homogeneous regions, the noise exists and need to be removed, though it is less visible. In order to improve the visual quality of the image, more low-pass filtering should be carried out in the homogeneous regions than in non-homogeneous regions. Hence, to make the noise removal effective with a good preservation of the signal variations, the filtering process should be performed with different kinds of low-pass operations. In general, the image can have three categories of regions. The non-homogeneous regions, where the gray level varies at higher frequencies, can have a light-dose of low-pass operation to remove some pitches if it is needed. A heavy-dose low-pass operation should be applied in obvious-homogeneous regions to remove the noise and artifacts. The rest of the image, of which some parts are close to the obvious-homogeneous regions and others to the non-homogeneous regions, may need median-dose low-pass filtering. Therefore, the filtering process is made to have several stages, as shown in Figure 3.2. The low-pass operations in the stages can be identical or different. The first stage, namely the pre-filtering, is made to perform a slight smoothing operation. The second one, i.e., LP_1, can perform a moderate or medium blurring. Assuming that all the stages, except the first one, have the same operator, the effective neighborhood size of the overall low-pass operation will increase from stage by stage, and the strength of the low-pass filtering will progress.

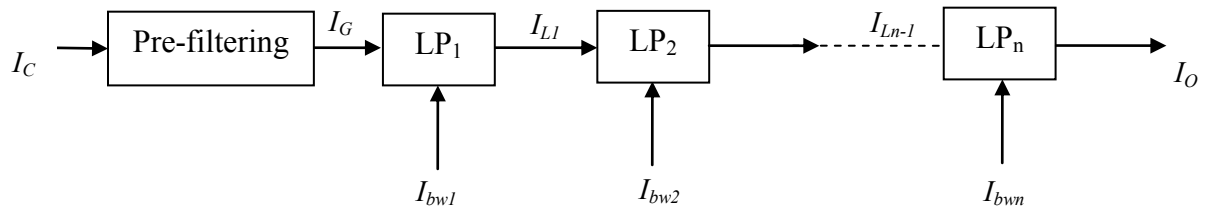

Figure 3.2 Different stages of the proposed discriminative filtering process. The masks $I_{bw1}, \ldots, I_{bwn}$ are used to make each operation to be applied to the selected pixels.

The low-pass operation in the first stage, i.e. a pre-filtering, is applied to the entire image, and that in each of the other stages is applied discriminatively to certain regions, defined by the mask I_{bwi}, as shown in Figure 3.2. Each of the masks makes a certain number of pixels exposed to receive the low-pass operation, and remaining ones masked to be untouched. If n_{pi} denotes the number of the exposed pixels in the mask I_{bwi}, we will have $n_{p1} \geq n_{p2} \geq . . . . \geq n_{pn}$. It is to say that the low-pass filtering is applied progressively, first to all the pixel population of the image, then to a large number of pixels, excluding those in obvious non-homogeneous regions, and in the last stage only those located in obvious-homogeneous regions will be processed.

As the progressive low-pass filtering is applied to make the pixels in different regions get different degree of smoothing, one needs to classify the pixels and grouping them according to the conditions of particular regions. As mentioned above, there are at least three categories of regions, i.e. obvious-homogeneous regions, non-homogeneous regions and the remaining ones. For a higher quality de-noising, the third category can be further divided. The criteria to be used in the classification are defined according to the applications and the critical issues in each detection. In this work, the classification is done in two steps, namely thresholding and region correction. The former is a coarse classification based on the pixel population condition and its result is fine- tuned in the latter.

Summarizing the above description, the proposed contrast enhancement can be expressed by the block diagram shown in Figure 3.3. The removal of noise and artifacts generated in the HE is done by a discriminative low-pass filtering process. The successive low-pass stages make the strength of the filtering progressive. The masks controlling each of the stages make the filtering discriminative in the image space and the different coverages by those masks allow the multiple-level low-pass filtering to be applied progressively in different categories of regions.

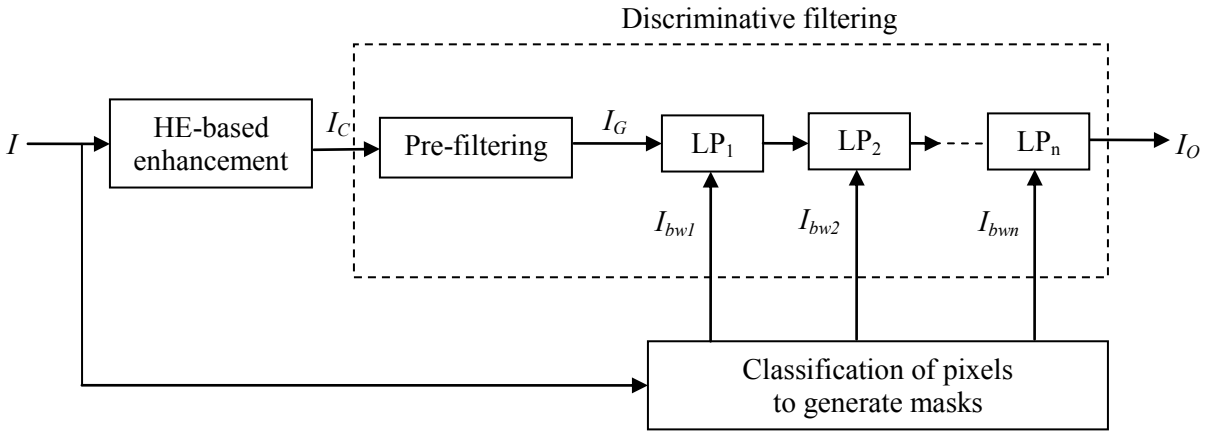

Figure 3.3 Block diagram of the proposed method of contrast enhancement followed by the low-pass filtering.

The input image used in the development is shown in Figure 3.4(b), referred to as the test image. It is obtained from the image in Figure 3.4(a), referred to as the reference image. The test image has a good combination of a flat background and multiple objects containing various frequency components of different orientations. Also, there are low contrast regions in both ends of gray level range, which is confirmed by its histogram shown in Figure 3.4(c).

(a) (b)

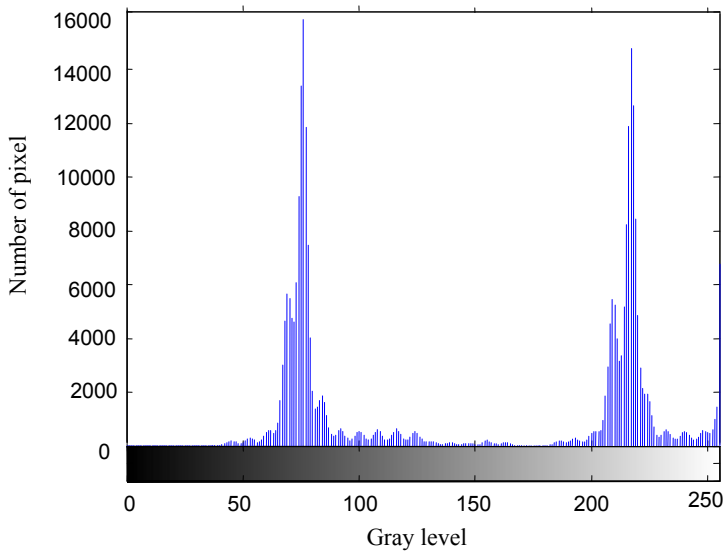

(c)

Figure 3.4 (a) Original good contrast reference image.
(b) Low contrast test image.
(c) Histogram of the test image.

3.2 Contrast enhancement by CLAHE

HE-based algorithms are widely used for contrast enhancement. The HE algorithm used in our scheme is Contrast Limited Adaptive Histogram Equalization (CLAHE) [1] , one of the commonly used adaptive HE algorithms. It provides users with a control of the degree of enhancement by means of the clip limit. A higher value of the clip limit results in a higher degree of contrast enhancement, however, also causes more visible noise and artifacts, particularly in homogeneous regions. Figure 3.5 illustrates two enhanced images and their histograms obtained by applying two different clip limit values, respectively.

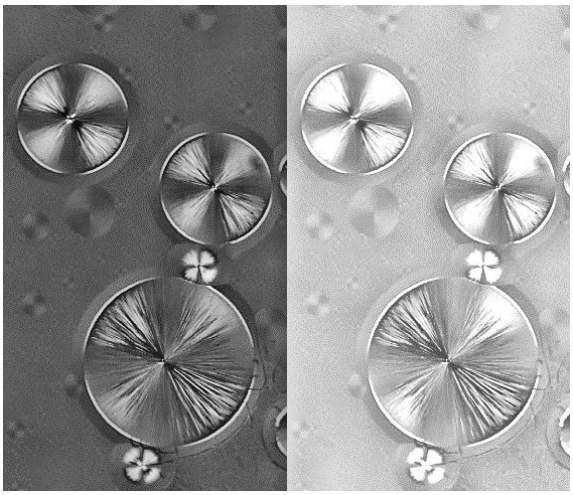

(a)

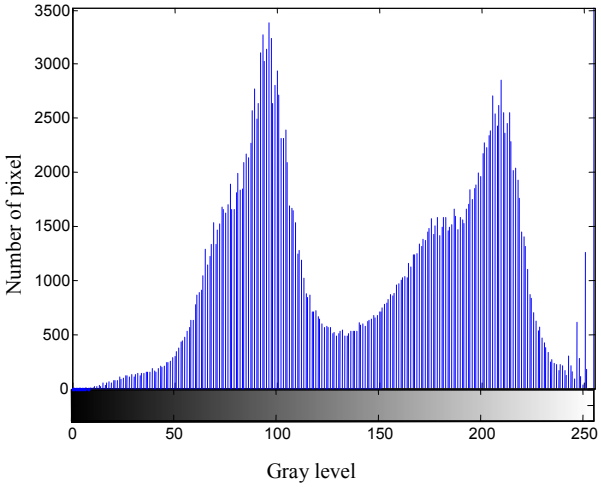

(b)

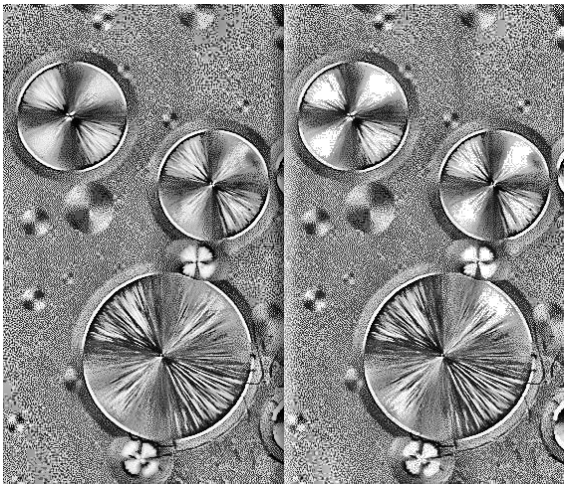

(c)

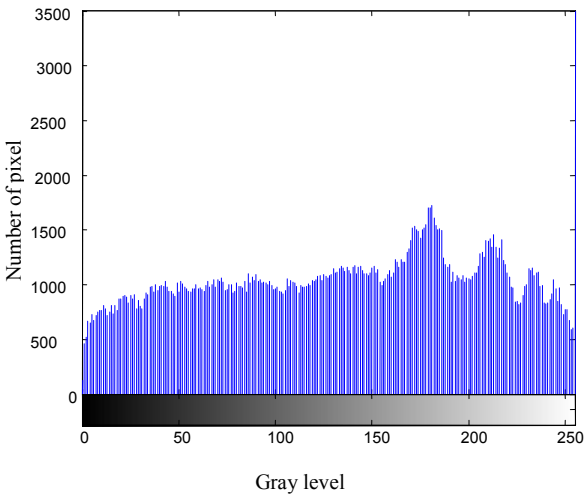

(d)

Figure 3.5 Images and their histograms obtained by applying CLAHE with different clip limit values. The tile size is 20x20.
(a) Clip limit: 0.01.
(b) Histogram of (a).
(c) Clip limit: 0.25.
(d) Histogram of (b).

Comparing the two enhanced images shown in Figure 3.5(a) and (c), one can easily see that the higher clip limit yields a better contrast enhancement as more details appear in Figure 3.5(c) than that in (a). However, the noise and artifact in Figure 3.5(c) is much more pronounced than that in (a). A better enhancement result of a higher clip limit is also reflected by a more even distribution of gray levels in the histogram as shown in Figure 3.5(d) than that in (b).

In the proposed method expressed in Figure 3.3, CLAHE with a high clip limit is used in the block of the HE-based enhancement as it enables to reveal more image details. The noise and artifacts resulting from this enhancement, however, requires a challenging task of their removal in the succeeding stages. In general, a low-pass filtering process is used for noise removal. But a good quality of removal operations necessitates a custom design to make the filtering suit the characters of the signal and the noise in order to preserve the image information. For this purpose, it's important to investigate the behavior of the noise introduced by the HE so that one can design the first stage of the filtering aiming at removing the noise with the priority of well preserving the signal variation. The procedure of the pre-filtering is presented in the following section.

3.3 Pre-filtering of the CLAHE-enhanced image

The pre-filtering block is designed to perform a very light low-pass filtering in the entire image with the priority of preserving the signal variation. In order to do so, one needs to have a good analysis of the noise to find its characters.

In the process of the HE, a small gray level variation in a homogeneous region can be enhanced in such a way that its amplitude becomes as large as those of the signals in non-homogeneous regions. To identify the noise variations from the signal variations, let's have some observation of the enhanced image by CLAHE shown in Figure 3.6(a) that is copied from Figure 3.5(c). The details of a region covering a homogeneous segment and a non-homogeneous one are illustrated in Figure 3.6(b). For a comparison purpose, the same region before the enhancement is presented in Figure 3.6(c).

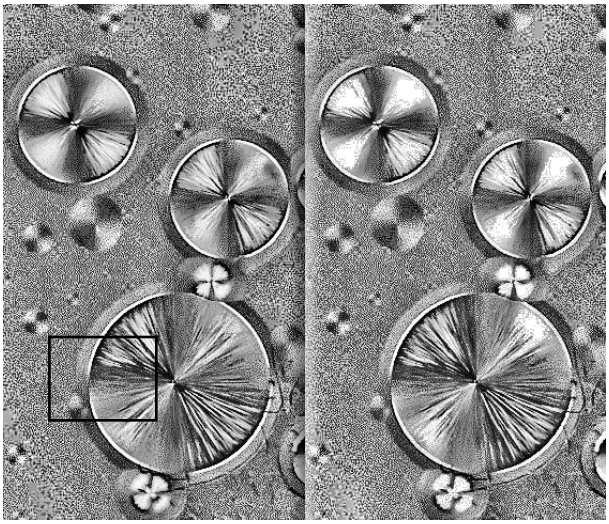

(a)

(b)

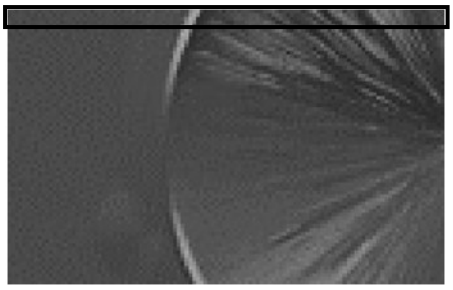

(c)

Figure 3.6 Comparison of the image segments before and after CLAHE process.
(a) Enhanced Image by CLAHE with clip limit: 0.25, The framed segment is shown in (b).
(b) Enlarged segment framed in (a).
(c) Enlarged segment before CLAHE process.

In Figure 3.6(b), the variations in the homogeneous segment have very noticeable appearance with respect to the signal details. However, it can be seen that the enhanced noise variations have some characters different from those of the signals. To better visualize the differences, a 1-D presentation of gray level variations sampled from the segments before and after CLAHE is shown in Figure 3.7.

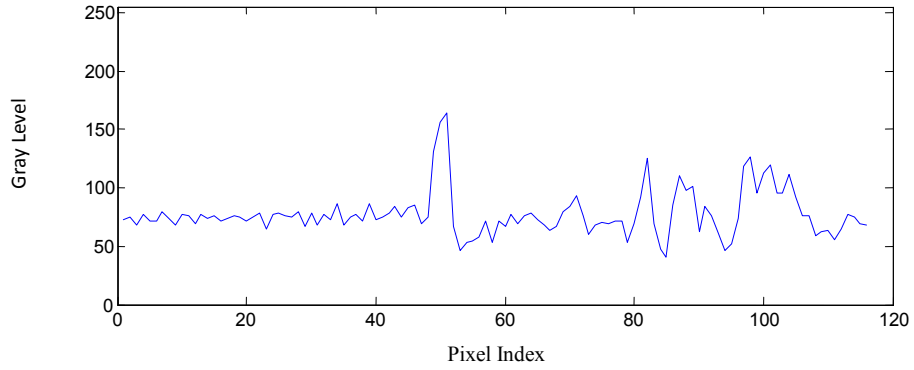

(a)

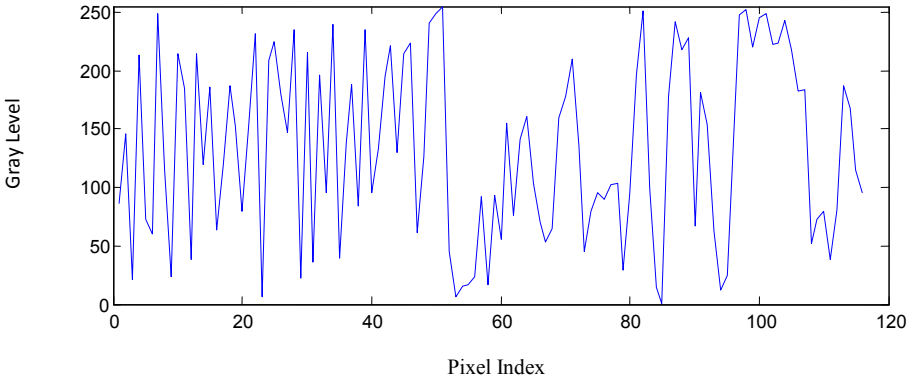

(b)

Figure 3.7 One-D presentation of the image samples.
(a) Before CLAHE, sampled from Figure 3.6(c).
(b) After CLAHE, sampled from Figure 3.6(b).

Each of the graphs in Figure 3.7 illustrates the gray level variations in both homogeneous and non-homogeneous segments. By observing the two graphs carefully, one can notice that the gray level variation of the noise in the homogeneous segment located in the left-hand side is very much enhanced and its frequency is visibly higher than that of the variation in the non-homogeneous segment. In this case, a low-pass filter can be used to filter out the high frequency noise. A simple Gaussian filter can be employed for this purpose. Figure 3.8(b) and (c) show the results of the Gaussian smoothing with different σ values applied to the image shown in Figure 3.6(a). Their corresponding 1-D presentations are shown in Figure 3.9(b) and (c).

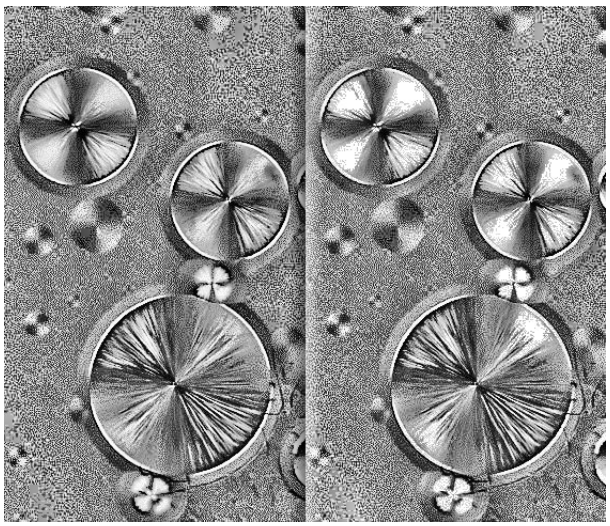

(a)

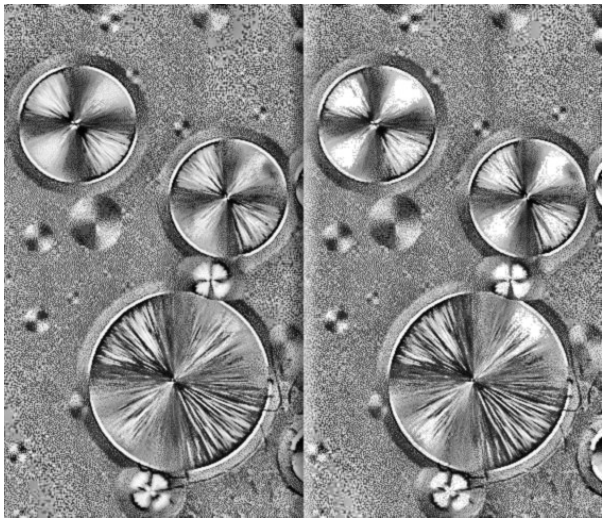

(b)

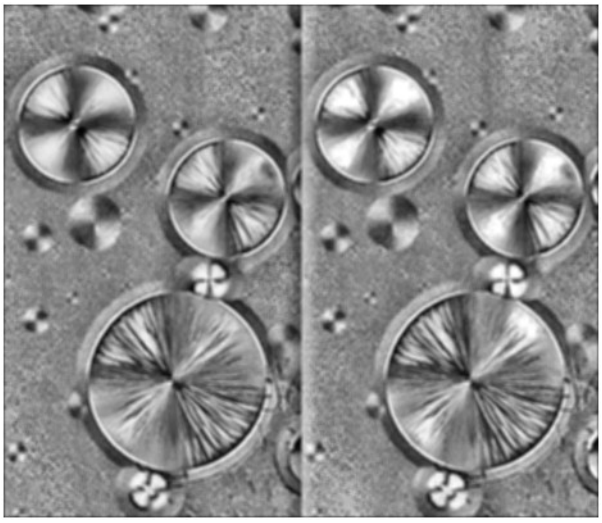

(c)

Figure 3.8 (a) CLAHE-enhanced image same as that shown in Figure 3.6(a).
(b) After Gaussian filtering with $\sigma = 0.6$.
(c) After Gaussian filtering with $\sigma = 2$.

By comparing Figure 3.8(b) and (c) with that shown in Figure 3.18(a), we see that in both of the smoothed images the noise in homogeneous regions is reduced. However, in Figure 3.8(b), more signal variations are preserved while its homogeneous region is less smoothed, compared

to those in Figure 3.8(c). As it is difficult to recover a signal detail once it is lost, an over-blurring filtering, as that observed in the non-homogeneous regions in Figure 3.8 (c), should be avoided in this stage. It should also be noticed that the image patterns in the non-homogeneous regions in Figure 3.8(b) look better than those in Figure 3.8(a), because the high frequency pitches are removed by the Gaussian filtering. Thus, a light smoothing is suitable in many cases as a pre-filtering applied to both homogeneous and non-homogeneous regions before the discriminative low-pass operations, in which the non-homogeneous pixels will be masked.

An 1-D presentation of the gray level variations at the same location as that in Figure 3.6 is found in Figure 3.9. It confirms that the higher σ Gaussian filtering causes a loss of some gray level details in non-homogeneous segments even though it makes a better noise removal in homogeneous segments.

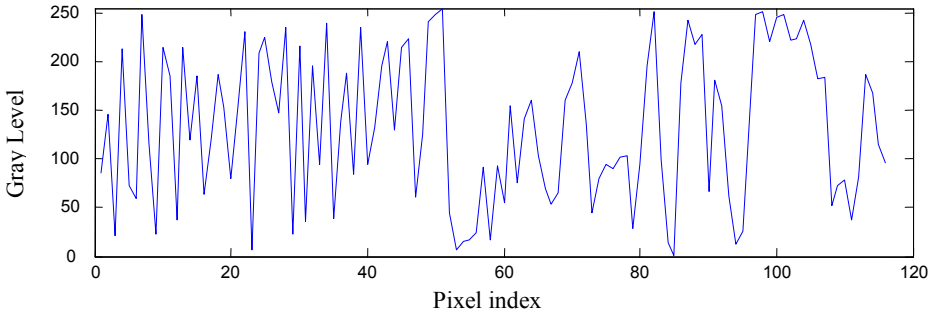

(a)

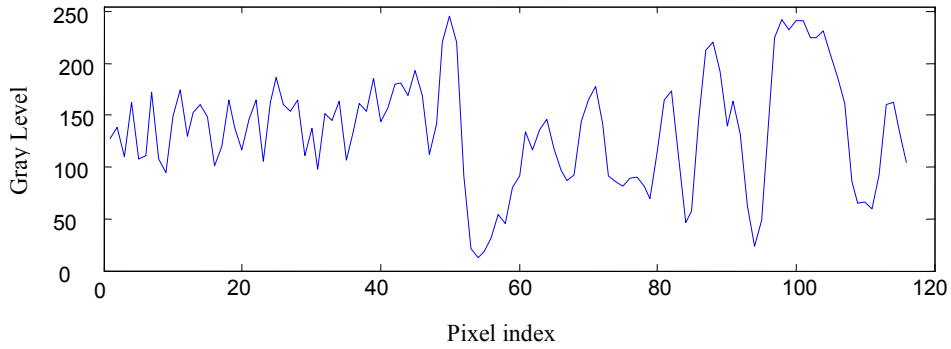

(b)

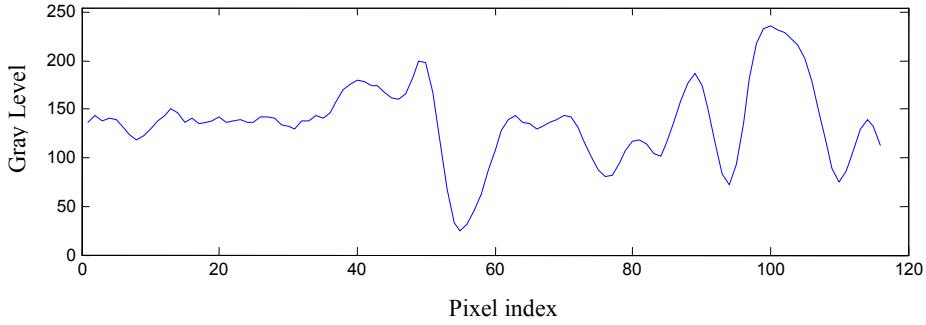

(c)

Figure 3.9 Comparison of image samples with-and-without Gaussian smoothing after CLAHE process.
(a) Image sample from Figure 3.5(c), before Gaussian filtering.
(b) Image sample from Figure 3.8(b) which is Gaussian-filtered with $\sigma = 0.6$.
(c) Image sample from Figure 3.8(c) which is Gaussian- filtered with $\sigma = 2$.

Based on this observation, it can be concluded that a Gaussian smoothing filter with a low σ can be used to carefully remove part of the HE-generated noise and artifacts. However, a better noise removal needs a low-pass filtering that has a discriminative nature in order to better smooth homogeneous regions meanwhile preserving the image details of non-homogeneous regions.

In the proposed method shown in Figure 3.3, a Gaussian filter with a very moderate or low σ value is used for the pre-filtering. The σ value of the Gaussian filter is determined in such a way that it only suppresses the noise that has much higher frequencies than those of the signals. In some cases, if the frequency difference is not significant, one may spare the pre-filtering in order to preserve the signal variations. Removing the noise and the artifacts that are not eliminated by the pre-filtering requires a further filtering process controlled by a signal I_{bwi} of classification as shown in Figure 3.3. To this end, this classification is to identify the pixels in homogeneous regions and non-homogeneous regions, as the noise in the homogeneous regions is mostly generated by the HE. In the following sections, more study of the characters of the gray level variations in these regions is presented and a procedure for classification is proposed.

3.4 Classification of the pixels and the generation of the masks

The pre-filtering presented in the previous section is designed to reduce the high frequency noises with a maximum preservation of signal variation and produces a filtered signal I_G. But the remaining noises and artifacts are still visible particularly in the homogeneous regions. Hence, in order to remove them, it necessitates a discriminative filtering process effectively functioning only on the homogeneous regions while keeping the pixels in non-homogeneous ones untouched.

To perform this filtering, an effective classification of the pixels in homogeneous regions, referred to as homogeneous pixels, and those in non-homogeneous regions, referred to as non-homogeneous pixels, is required. The result of the classification process is used to create binary masks, in each of which the two logic levels '0' and '1' represent the pixel positions in the non-homogeneous and relatively homogeneous regions, respectively. Each of these binary masks is used to shield non-homogeneous pixels of the pre-filtered or filtered image from the low-pass operation in one of the stages while the gray level variations of the other pixels are smoothed.

3.4.A Distribution of homogeneous and non-homogeneous pixels in the histogram

A histogram indicates the gray level distribution in an image and can be used to classify the pixels [3]. In this design, the classification is to distinguish pixels of the homogeneous regions from the entire population. It is known that the pixels in homogeneous region can form high peaks in the histogram. Hence the design of the classification procedure starts with an observation of these pixels.

The histograms of the three images available in this stage, namely I the original image, I_C produced by CLAHE and I_G resulting from the pre-filtering, are presented in Figure 3.10. Among them only that of the original one shown in Figure 3.10(a) illustrates clearly two peaks corresponding to two groups of the pixels in the homogeneous regions at the upper and lower sections of the gray level range. Most pixels in the high bins belong to homogeneous regions. In the original image, the gray level of a pixel gives, more or less likely, an indication, in which categories of regions it is located. The relevance between a pixel location and the gray level may

be lost after a filtering or enhancement. Hence, the analysis is based on the histogram of the original image.

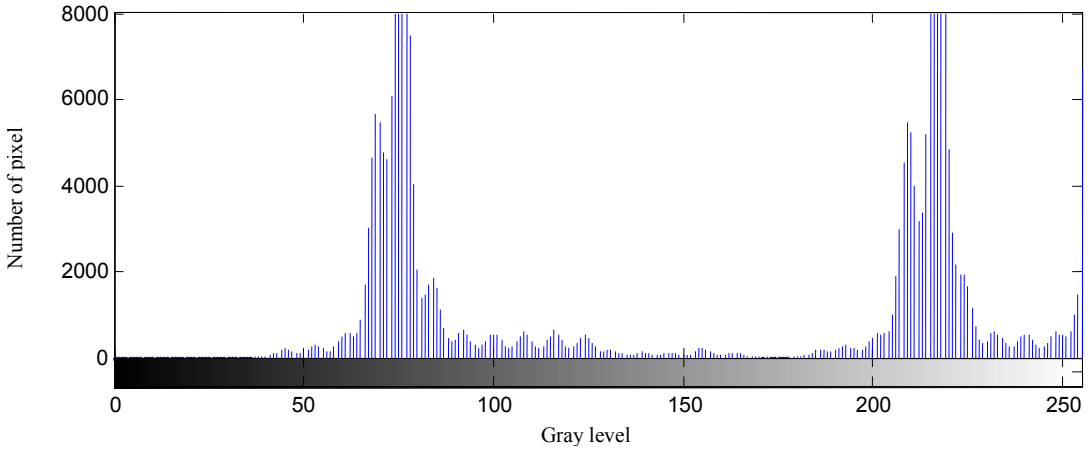

(a)

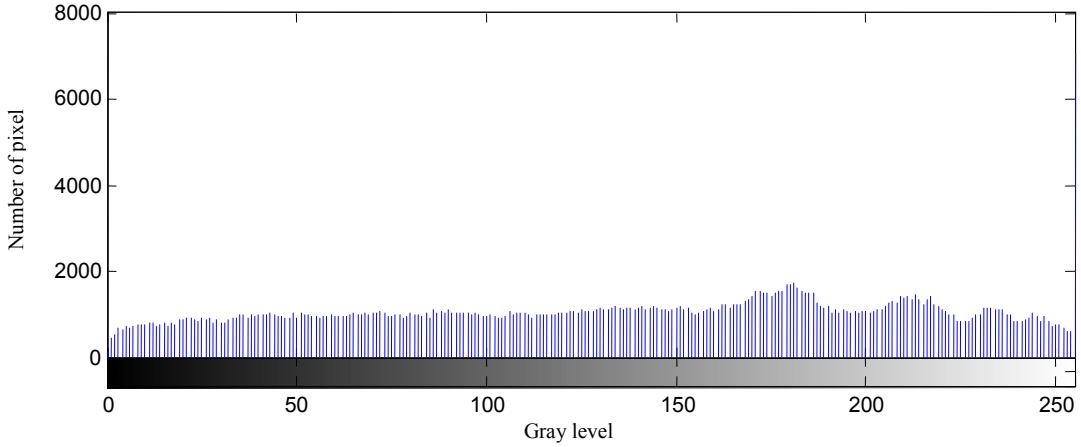

(b)

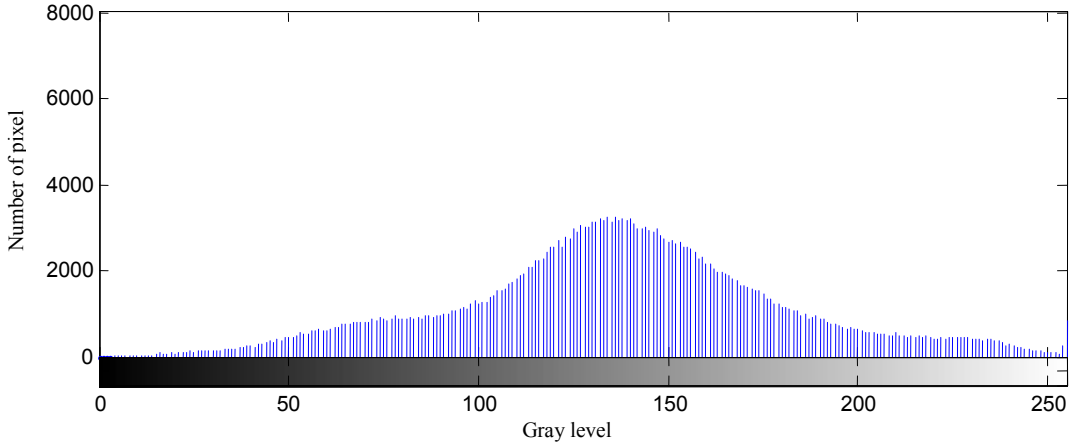

(c)

Figure 3.10 (a) Histogram of the original image.
(b) Histogram of the contrast enhanced image.
(c) Histogram of the pre-filtered image.

Let us have a close observation of the above-mentioned relevance shown in the histogram of a low contrast image illustrated in Figure 3.11. It is similar to the lower section of that shown in Figure 3.10(a). The peak indicates the existence of homogeneous regions. There is a very high concentration of homogeneous pixels in the bins around the gray level G_{peak}. The more distant from G_{peak}, the less the concentration is. In other words, the concentration of the pixels from non-homogeneous regions increases with the distance from it.

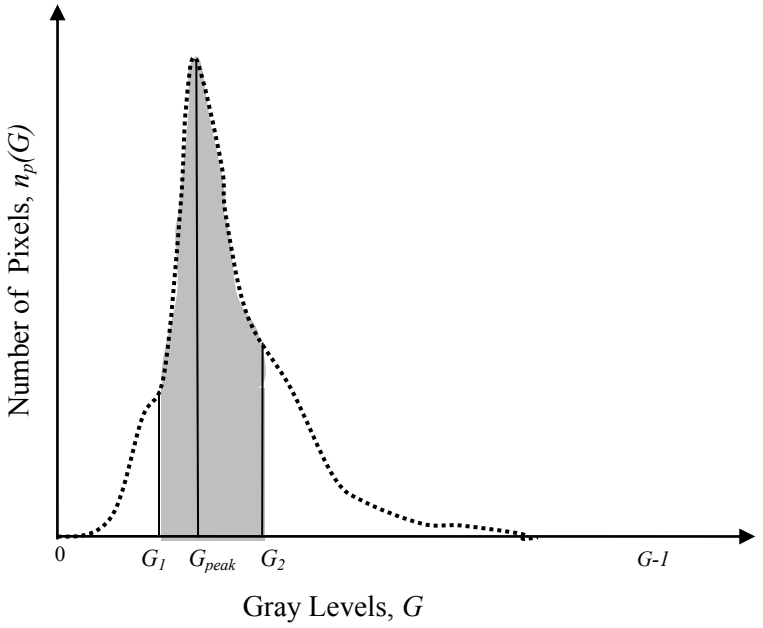

Figure 3.11 Histogram of a low contrast image. Most of the pixels in the shaded area are likely from homogeneous regions and the majority pixels in the other parts, i.e., those not shaded, are from non-homogeneous regions.

In Figure 3.11, the pixels in the shaded area can be classified as homogeneous pixels and those in the remaining areas as non-homogeneous pixels with a certain rate of misclassification.

If n_{total} denotes the total number of the pixels classified as homogeneous ones and n_{miss}, the number of pixels from non-homogeneous regions but included in n_{total}, the misclassification rate will then be $\frac{n_{miss}}{n_{total}}$. The optimal classification is to maximize n_{total} while minimizing n_{miss}. The values of n_{total} and n_{miss} are related to how close the boundaries G_1 and G_2 are to G_{peak}. One can choose G_1 and G_2 to define the shaded area precisely. In this case, n_{miss} can be reduced by reducing $|G_2\text{-}G_1|$, as the concentration of the pixels from homogeneous regions is relatively higher in the bins closer to G_{peak}. However, narrowing the shaded area, i.e. smaller $|G_2\text{-}G_1|$, also reduces n_{total}, making more homogeneous pixels classified as non-homogeneous ones. Thus, the shaded area defined by a small value of $|G_2\text{-}G_1|$ interprets as a low risk of misclassification of pixels from non-homogeneous regions, but a high risk of that of pixels from homogeneous regions. On the contrary, if the value gets larger, the effect will be in the opposite direction. It is thus difficult to achieve a good classification by a simple thresholding in the histogram with a set of G_1 and G_2 values.

The above described phenomenon can also be observed in a gray level presentation in image space. Figure 3.12 illustrates 1-D gray level variations of a sample from the low contrast image, assuming that the variations in the left segment are of noise and those in the right segment of signal. It is visible that in this sample, the number of pixels, of which the gray level is equal to G_{peak} or close to it, is relatively large, which is coherent to the peak appearing in the histogram shown in Figure 3.11. This 1-D presentation visualizes the choice of G_1 and G_2, the gray level boundaries, with respect to the degree of the risk of misclassification. In Figure 3.12(a), the two values are set in such a way that the range (G_{1H}, G_{2H}) covers the maximum number of the pixels in the homogeneous regions. But, this range also includes a good number of pixels located in the non-homogeneous regions. So, this set of G_1 and G_2 would result in a high n_{miss}. Contrarily, if

$|G_{2-} G_1|$ is made much smaller, as $|G_{2L} - G_{1L}|$ shown in Figure 3.12(b), a smaller number of pixels will be covered in both regions. In this case, on one hand, a much smaller number of pixels in the non-homogeneous regions will be included, thus reducing the risk of misclassifying the pixels in this region. On the other hand, some of the pixels from the homogeneous regions will be missed, i.e. excluded from the shaded area in the histogram.

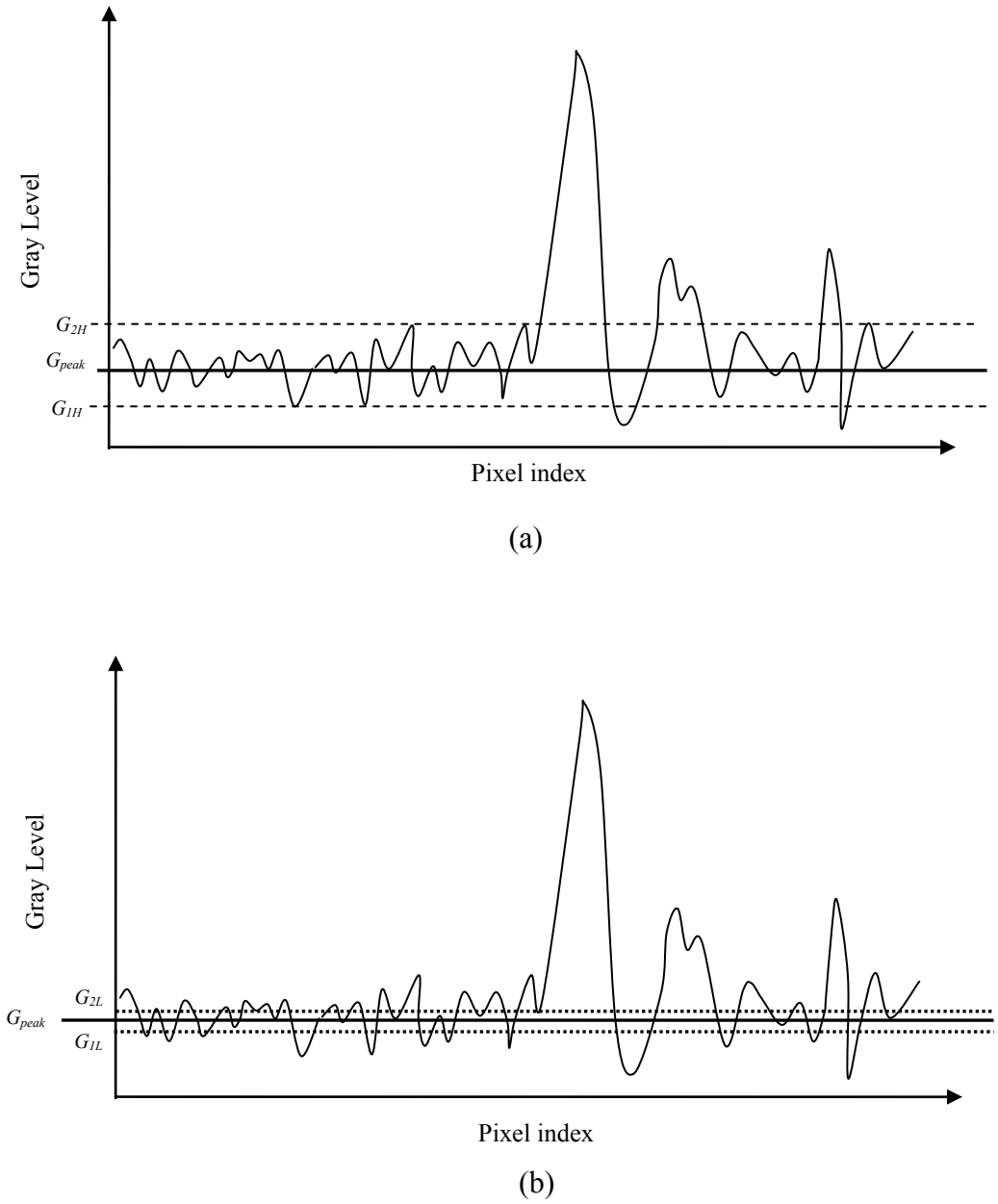

Figure 3.12 One-D presentations of a segment of a low contrast image. The variations in the left side are more likely to be of noise while that in the right side of signal. The gray level G_{peak} corresponds to the histogram peak as that shown in Figure 3.11.
(a) Large $(G_2\text{-}G_1)$.
(b) Small $(G_2\text{-}G_1)$.

There can be two types of consequences following the misclassifications. If the misclassification is such that homogeneous pixels are misclassified as non-homogeneous pixels, they will be masked during the low-pass operation and thereby, the gray level variations, likely produced by noise, in these pixel positions will not be removed. On the other hand, if non-homogeneous pixels are misclassified as homogeneous ones, the gray level variation that is likely of image signals will be erased by the low-pass filtering, resulting in a loss of information. As it is difficult to recover the information once it is lost, it is reasonable to avoid a misclassification of pixels that belong to the non-homogeneous regions.

From the observation described above, one can see that the classification, by means of grouping the pixels on the basis of G_1 and G_2 in the histogram, is far from satisfactory. Thus, the classification needs more precision than what this kind of method can lead to. The proposed classification of the pixels of the original image comprises two steps, as shown in Figure 3.13. The first step is to group the pixels in a coarse manner, by means of the histogram thresholding as illustrated in Figure 3.11 to produce the binary image I_{bw}'. The emphasis in the design of this step will be the minimization of the misclassification of pixels that belong to the non-homogeneous regions to reduce the risk of erasing signal variations. By this minimization, some pixels in homogeneous regions may be classified as non-homogeneous pixels. Thus, the next step, i.e. the region correction, should be designed to identify these misclassified pixels in the homogeneous regions and once identified, their status should be changed to that of the homogeneous region group. In the following sections, the design of each step will be presented.

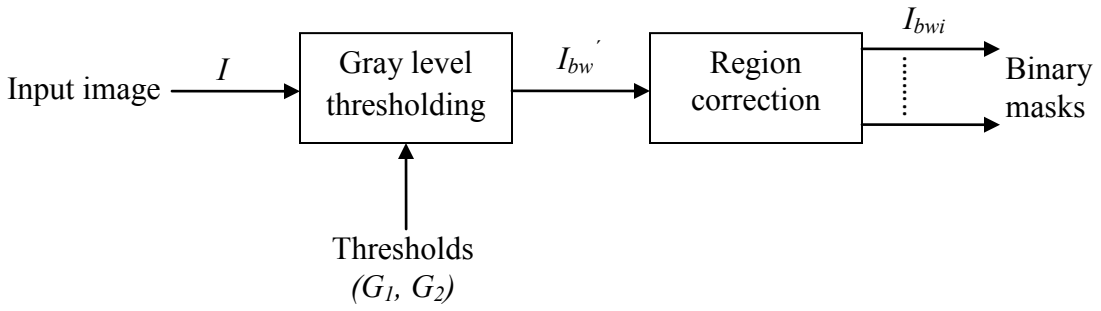

Figure 3.13 Classification process with multiple steps

3.4.B Gray level thresholding

The first step is to group the pixels by thresholding with two gray levels, namely G_1 and G_2 as shown in Figure 3.11. By means of this step, the signals of the pixels are binarized. If the gray level of a pixel is between G_1 and G_2, it will be classified as a homogeneous pixel, having its status presented by logic '1', otherwise a non-homogeneous pixel with logic '0'. The thresholding operation results in the binary mask I'_{bw} and can be simply expressed as follows,

$$I'_{bw}(i,j) = \begin{cases} '1' & if \quad G_1 \le I(i,j) \le G_2 \\ '0' & otherwise \end{cases}$$

The threshold values of G_1 and G_2 should be chosen with two limits set up on the basis of the observation of the image. The first limit is related to the minimization of the misclassification of the pixels located in non-homogeneous regions in order to preserve the signal variation in these regions. To this end, the gray level range defined by G_1 and G_2 should be as close to G_{peak} as possible, which can be visualized by the 1-D presentations shown in Figure 3.12. However, if the range is too small, a large number of pixels in homogeneous regions will be misclassified, and

there must be another limit for it. Figure 3.14 illustrates the test image, and two binary images obtained with two sets of (G_1, G_2), respectively. In the binary images, the black segments are composed of '0' pixels, i.e. the pixels classified as non-homogeneous ones, of which some are truly homogeneous pixels but misclassified. In Figure 3.14(b), the patterns of the black segments composed of misclassified pixels in the homogeneous background look identifiably different from those of truly non-homogeneous regions. Figure 3.14(c) is obtained with much smaller value of $|G_1-G_2|$, and consequently a much larger number of pixels in homogeneous regions are misclassified, which makes an identification of the patterns formed by the misclassified pixels hardly possible.

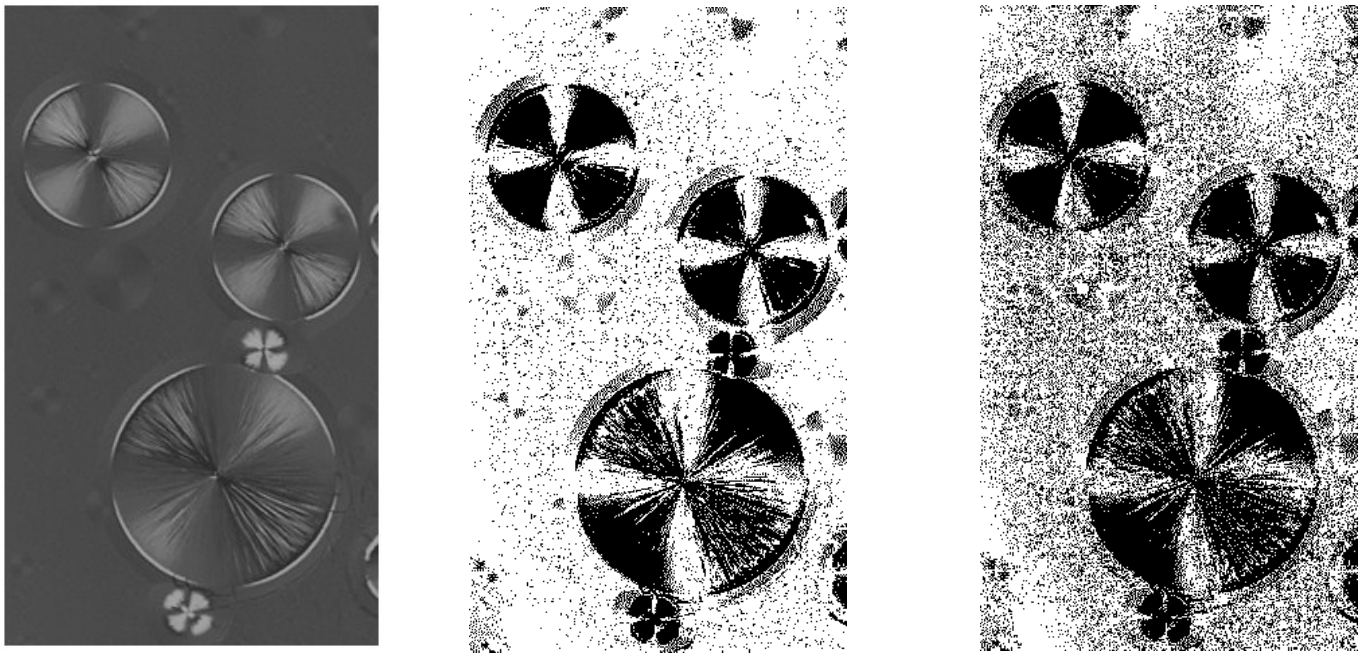

(a) (b) (c)

Figure 3.14 (a) Darker half of the test image with G_{peak} = 76.
(b) Binary image produced by thresholding with G_1 = 67 and G_2 = 79.
(c) Binary image produced with G_1 = 73 and G_2 = 78.

This thresholding operation is not to create a final mask, but a binary image prepared for the fine-tune classification. The images to be processed may have different critical issues depending on their applications. In some cases, signal details in a particular range of gray levels or of signal variation frequency, have more priority to be enhanced than those in other ranges, and these issues should be taken into considerations in choosing G_1, G_2 values to optimize the results.

3.4.C Region correction

The second step, namely region correction, is to correct the status of homogeneous pixels that are wrongly classified as non-homogeneous pixels. As the threshold values G_1 and G_2 in the first step are chosen to minimize the misclassification of the pixels in non-homogeneous regions, a significant number of homogeneous pixels may be misclassified as non-homogeneous ones and the correction thus aims at these pixels. If they are not corrected, the logic '0' value in these pixel positions will mask the noise and artifacts from the low-pass filtering. It should be underlined that the region correction is made to generate, from the binary image produced by the thresholding, masks to be used in different stages of the progressive low-pass filtering.

To correct the status of the homogeneous pixels which are wrongly classified as non-homogeneous ones, one needs to differentiate the patterns formed by likely true non-homogeneous pixels and those of misclassified ones. It is known that a true non-homogeneous region is unlikely to be one-pixel-wide. In the binary image I'_{bw}, if a region of non-homogeneous pixels is very thin, e.g. only one-pixel-wide, it is likely to be formed by misclassified pixels. Thus, the status of all these pixels should be corrected from '0' to '1'.

The one-pixel-wide regions in the binary image I'_{bw} can have different variations, in terms of orientation and connectivity of the segments. Figure 3.15 illustrates some of the simplest patterns segmented from one-pixel-wide regions and appearing in a 3x3 window. This kind of simple patterns is referred to as group-1. They are considered very likely formed by misclassified pixels located isolatedly in homogeneous regions and the correction of the pixels' status will be carried out to make a good low-pass filtering effective in the regions.

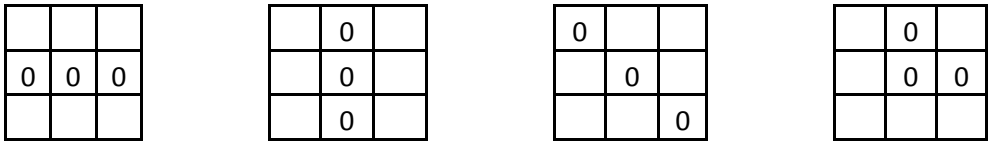

(a) (b) (c) (d)

Figure 3.15 Some of one-pixel-width patterns of group-1. The logic '0' indicates that the pixel classified as a non-homogeneous pixel. The blank spaces represent logic '1's. The other patterns in this group can be obtained by rotating, mirroring or shifting each of these four.

The patterns, referred to as group-2, are shown in Figure 3.16. They can also be seen as one-pixel-width, but have more variations than those in group-1. These patterns may be formed by misclassified pixels, but with a little less certainty compared to those in group-1. They are likely to be located close to non-homogeneous regions. In this case, it is appropriate to have a weak low-pass filtering to remove some noise with certain precaution.

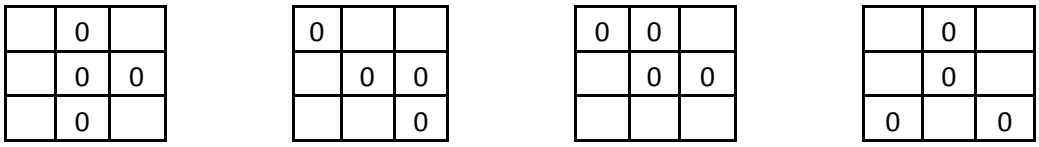

(a) (b) (c) (d)

Figure 3.16 Patterns of one-pixel-width segment of group-2. The form of the segment in each of the windows is less straight forward than those of group-1 shown in Figure 3.15. The other patterns in this group can be obtained by rotating, mirroring or shifting each of these four.

There are some other particular patterns, shown in Figure 3.17(a) and (b) featuring one-pixel-width. They are referred to as group-3. In general, this kind of patterns can be segmented from a region in which a logic '0' is found in every other pixel position as shown in Figure 3.17(c) or from the crossing of two one-pixel-width regions. In either case, the logic '0' pixels are likely to be misclassified ones and need to be corrected.

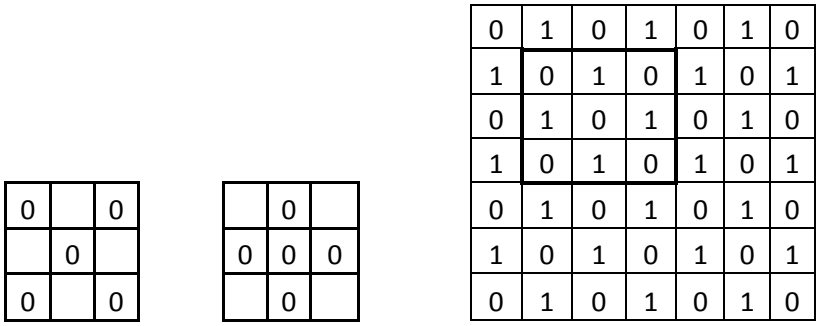

(a) (b) (c)

Figure 3.17 Special patterns referred to as group-3.

Summarizing the above-presented analysis on the patterns, one can conclude that the '0' status in the pixel positions in the patterns of all the three groups needs to be corrected to enable the operations of the low-pass filtering in these positions. The patterns of group-1 and group-3 are likely located in obvious-homogeneous regions where a high degree of low-pass filtering will be applied, whereas those of group-2 in less homogeneous regions in which a weak low-pass operation is needed without aggressive gray level variation removal.

As mentioned in § 3.1, different degrees of gray level smoothing is implemented by means of the progressive low-pass filtering in the successive stages. The mask to be used in the first stage, after the pre-filtering, should have the largest number of pixels, whose positions are of logic '1', i.e. not masked for the first low-pass filtering. They consist of those generated by the thresholding and those belonging to all the three groups. In the further stage of the low-pass filtering, only the pixels in the obvious-homogeneous regions should be exposed, i.e., excluding those in less homogeneous regions.

In the classification of the pixel positions, one needs to develop algorithms to identify the patterns in the three groups. In each of the algorithms, the first thing to do is checking the status of the input pixel. If it is logic '0', the status of the neighboring pixels in its 3x3 window will be examined to decide whether its logic '0' status should be corrected or not. This procedure is executed N^2 times for an image of NxN pixels to generate a new mask with more pixels of '1' status than that of the input I_{bw}'. The algorithms identifying the patterns of these three groups are described as follows.

3.4.C.1 Algorithms for the identification of the patterns

It can be observed that, in each of the patterns illustrated in Figure 3.15, the number of '0' pixels is equal to two. Thus, such one-pixel-width patterns or a section of it can be identified by simply counting the number of '0' pixels in the windows and comparing the result with two. If it is equal to or smaller than two, the correction of the status from '0' to '1' will be done. The algorithm of the identification of group-1 patterns and their correction is presented in Figure 3.18. In order to create the binary mask including the corrected pixels of group-1, the algorithm shown in Figure 3.18(a) will be performed repeatedly from the first pixel to the $(NxN)^{th}$ pixel.

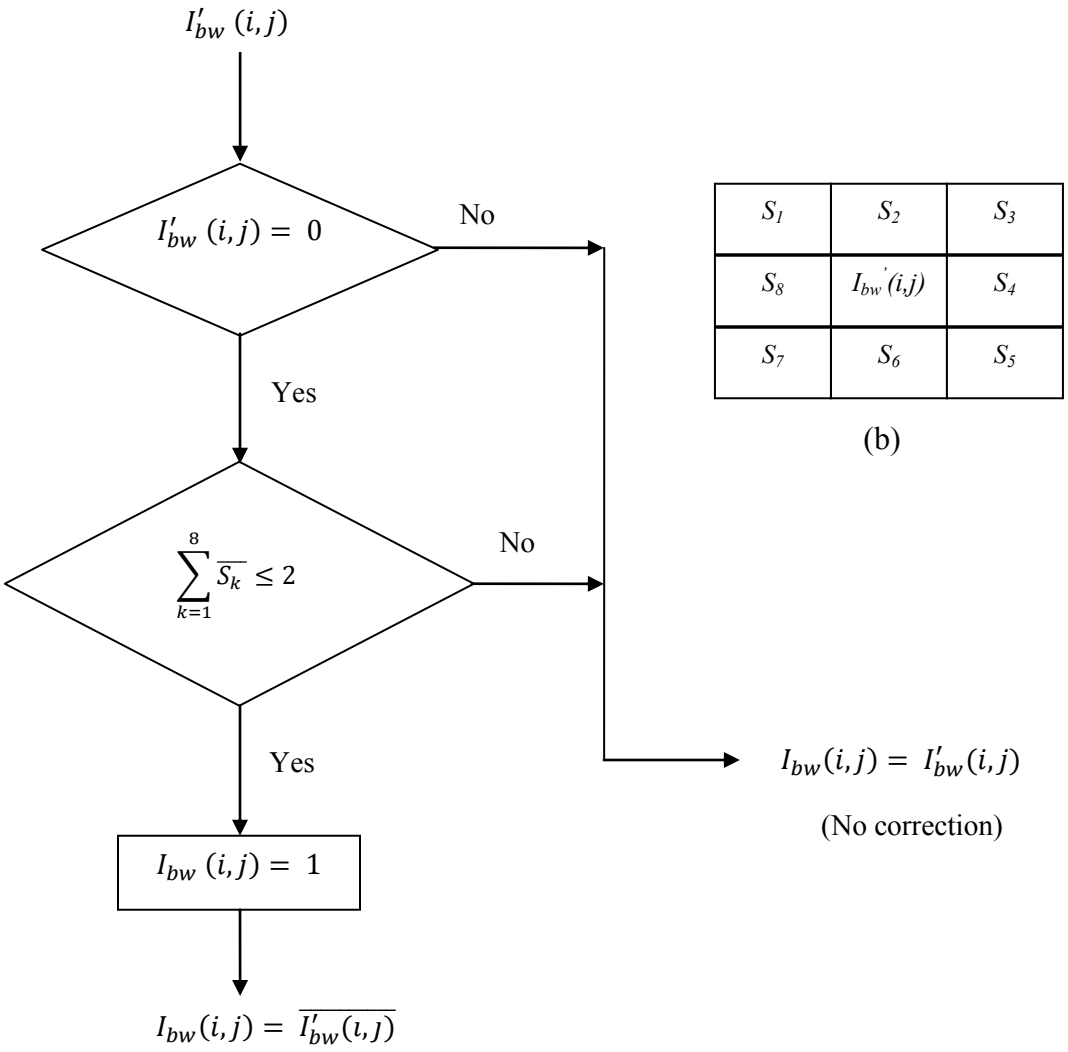

Figure 3.18 (a) Flow chart of the identification of the group-1 patterns and the subsequent decision concerning the correction of the status.
(b) A 3x3 window with the center pixel as $I_{bw}'(i,j)$ and S_k as one of the eight nearest neighbors with $k = 1, \ldots, 8$.

The patterns of group-3 shown in Figure 3.17(a) and (b) can be identified by a simple algorithm. Either of the two patterns of group-3 satisfies the conditions that the four corner pixels

have the same status, and the four remaining ones in the window is complementary to the corner ones. These conditions can be expressed as follows:

$$(i)\ S_1 = S_3 = S_5 = S_7\ , and$$

$$(ii)\ S_2 = S_4 = S_6 = S_8\ , and$$

$$(iii)\ S_{2m-1} = \overline{S_{2m}}\ ,\quad m = 1, 2, 3, 4.$$

where $S_1 \sim S_8$ represent the eight nearest neighbors of the pixel in question $I_{bw}'(i,j)$ as shown in Figure 3.19(b). The algorithm of the identification of the patterns of group-3 and the correction is shown in Figure 3.19(a).

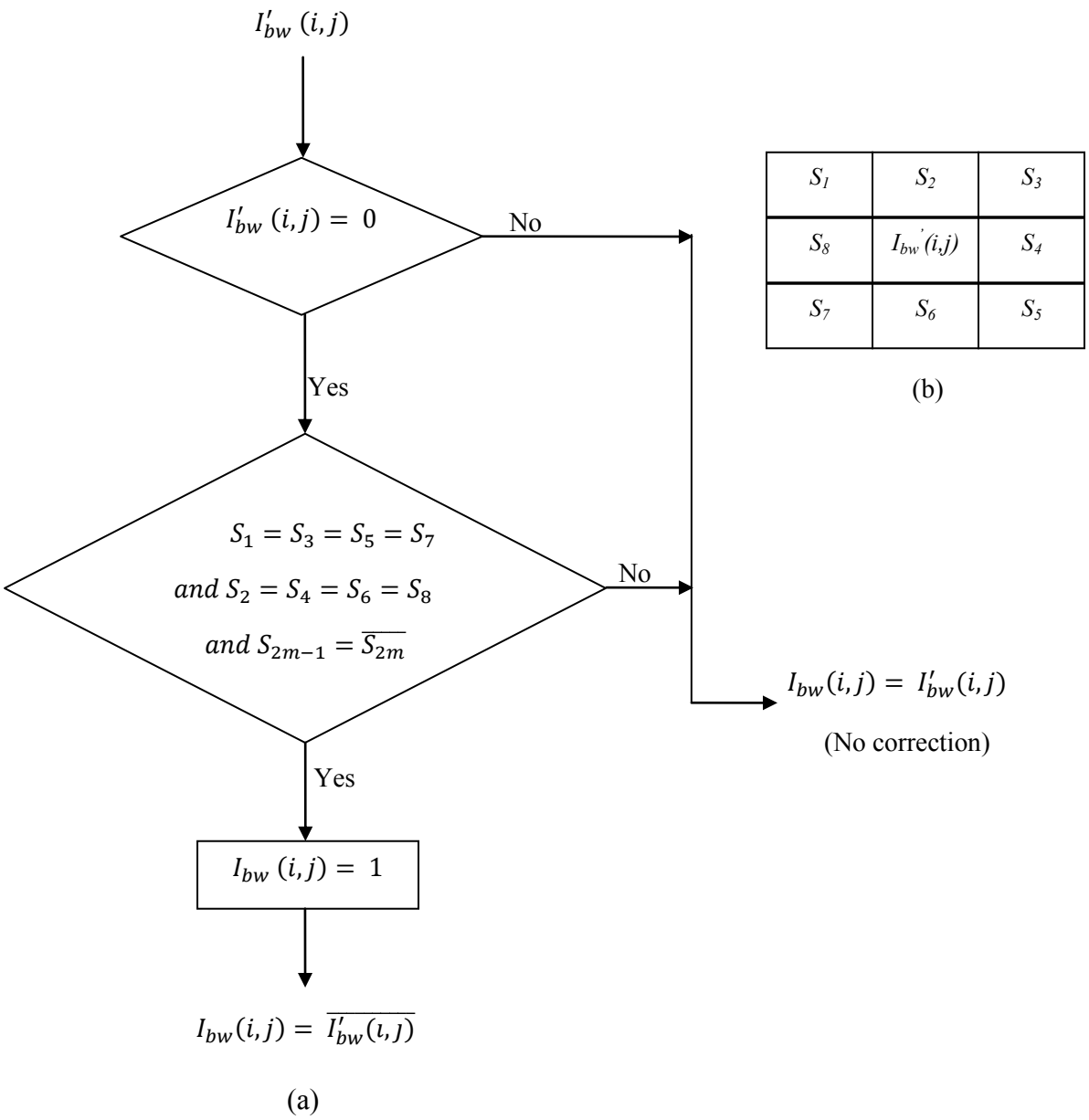

Figure 3.19 (a) Flow chart of the identification of the group-3 patterns and the subsequent decision concerning the correction of the status.
(b) A 3x3 window with the center pixel as $I_{bw}'(i,j)$ and S_k as one of the eight nearest neighbors with k =1, . . . , 8.

The patterns of group-2 shown in Figure 3.16, satisfy the condition that the number of surrounding pixels having the '0' status is equal to three. However, some patterns that do not belong to group-2 also satisfy this condition. Figure 3.20 illustrates these patterns, referred to as group-4. If the identification of the group-2 patterns is done by counting of the number and a comparison with the constant of 3, the patterns of group-4 should be detected and excluded. The algorithm of the identification of group-2 pattern and correction is shown in Figure 3.21.

It should be noted that if the comparison condition in this algorithm shown in Figure 3.21(a) is $\sum_{k=1}^{8} \overline{S_k} \leq 3$, instead of $\sum_{k=1}^{8} \overline{S_k} = 3$, the subsequent correction will also be effective to the pixels of the group-1 patterns. It should also be noted that in some cases it is not necessary to exclude the patterns of group-4 in the generation of a mask to be used in a medium-level smoothing operation and the algorithm shown in Figure 3.21 can be simplified.

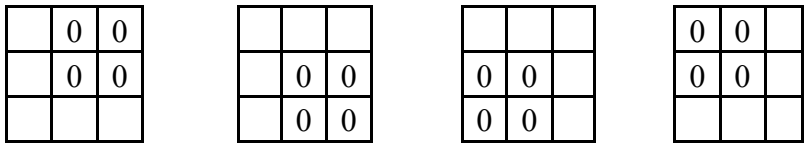

Figure 3.20 Patterns in which the number of the surrounding pixels having '0' status is equal to three, but do not belong to group-2.

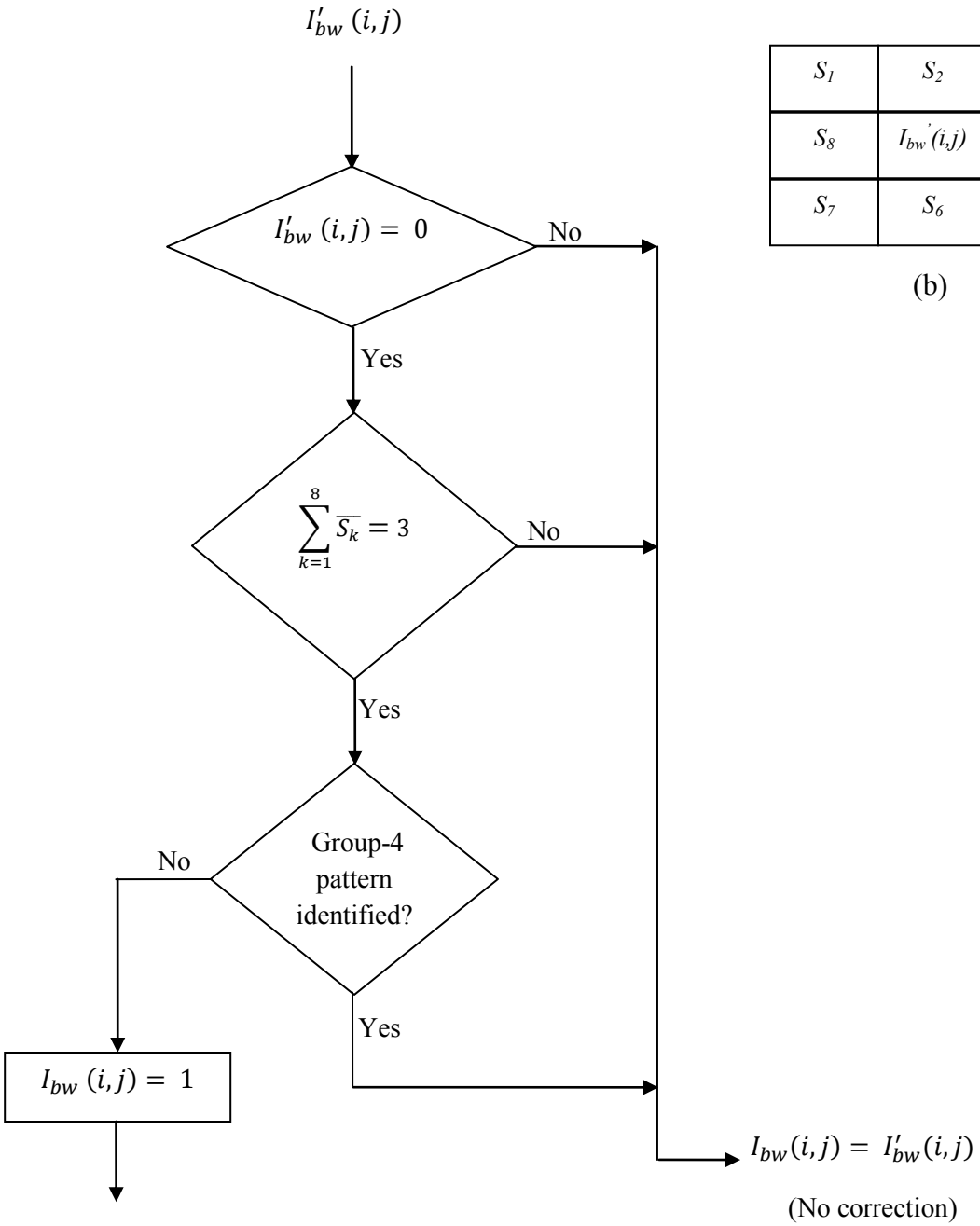

Figure 3.21 (a) Flow chart of the identification of the group-2 patterns and the subsequent decision concerning the correction of the status.
(b) A 3x3 window with the center pixel as $I_{bw}'(i,j)$ and S_k as one of the eight nearest neighbors with $k = 1, \ldots, 8$.

In the algorithm shown in Figure 3.21(a), the identification of the group-4 patterns shown in Figure 3.20 is based on the examination of each of the four corner pixels and its adjacent neighbors. If all of the three pixels, i.e. the corner one and the two neighbors have the '0' status, the center pixel $I_{bw}(i,j)$ will be identified as one in the group-4 patterns and thereby, its status will remain as '0'. The condition to detect the group-4 patterns, in this algorithm can be modeled as:

$$(i)\ S_{2m} = S_{2m+1} = S_{2m+2} = '0',\ \text{where } m = 1 \text{ or } 2 \text{ or } 3, \quad \text{or}$$

$$(ii)\ S_8 = S_1 = S_2 = '0'.$$

The algorithms presented in Figures 3.18, 3.19 and 3.21 will be used to generate the binary masks for the different stages of the progressive low-pass filtering. The approaches to generating the masks can be different, depending on the way the procedure is implemented. One of the approaches is presented in the following section.

3.4.C.2 Generation of the masks enabling different degrees of low-pass filtering

The binary masks needed in the progressive low-pass filtering process are used to provide multi-level protection by shielding different groups of pixels from different degree of gray level variation removal. In the first stage, after the pre-filtering, of the proposed low-pass filtering, the gray level variation removal is applied to all the pixels in homogeneous regions. In other words, the binary mask used in this stage should make all the homogeneous pixels identified by the thresholding or by the region correction open to the low-pass operation. The mask can be

generated by the procedure illustrated in Figure 3.22. It involves the correction of the pixels belonging to group-1, 2, 3 and 4 patterns. In some cases, the exclusion of patterns of group-4 may be needed, the logic operations identifying these patterns will be incorporated in the procedure.

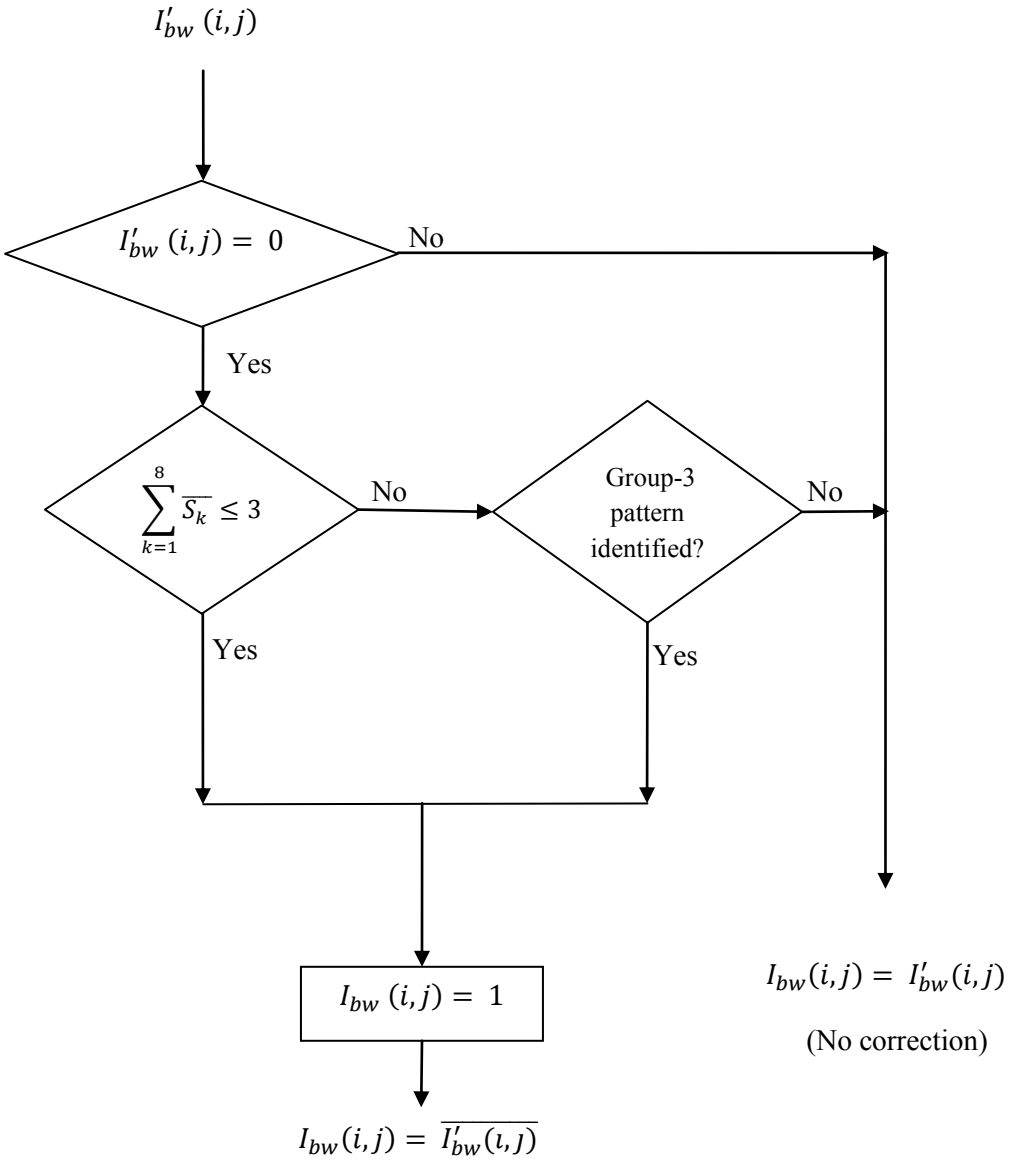

Figure 3.22 Flow chart of the generation of the binary mask for the first stage of the proposed low-pass filtering.

The further gray level variation removal in the second stage of the low-pass filtering is applied only to the obvious-homogeneous regions. The mask used in this stage will protect the non-homogeneous regions and less-homogeneous regions, i.e., those adjacent to non-homogeneous regions. Thus, the pixels of logic '1' in this mask are those identified by the thresholding or by the correction of group1. The mask can be created by the procedure illustrated in Figure 3.23 which is same as the procedure shown in Figure 3.18.

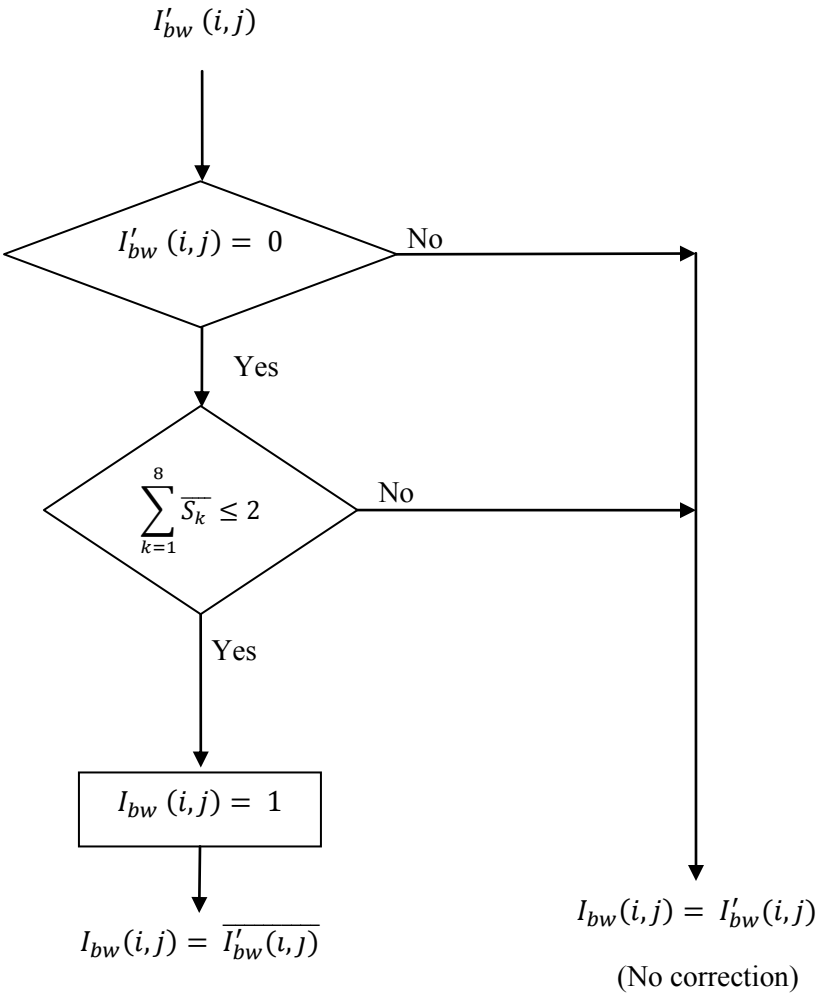

Figure 3.23 Flow chart of the generation of the binary mask for the second stage of the proposed low-pass filtering.

Incorporating the procedures shown in Figure 3.22 and 3.23, the generation of the masks for the low-pass filtering can be presented in Figure 3.24. It should be noted that the progressive low-pass filtering may have the number of stages more than two if more precision is needed in the process, and thus may need more masks. The protection provided by the masks may need to vary according to the applications. Hence, the designs of the masks should have different critical issues to detect different patterns.

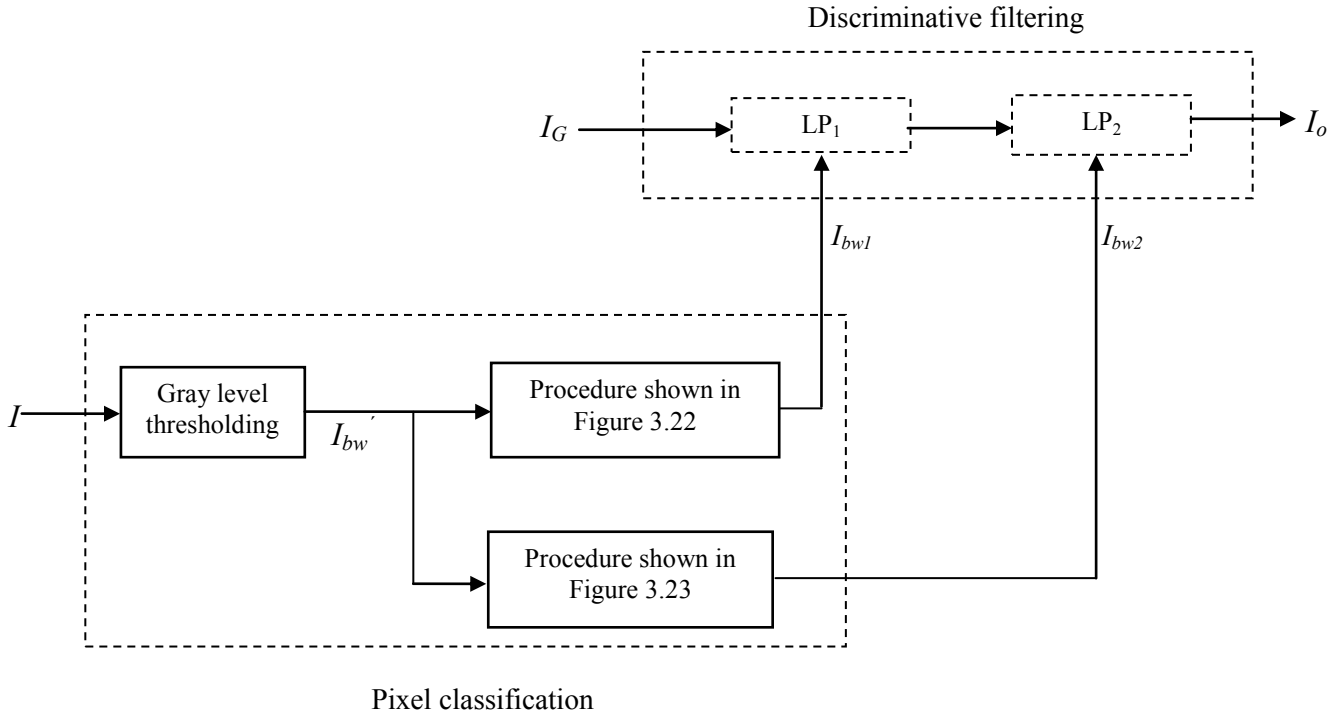

Figure 3.24 Generation of the binary masks for the application in the low-pass filtering. Here I_{bw1} and I_{bw2} denote the two binary masks produced by the procedures shown in Figure 3.22 and 3.23, respectively.

Figure 3.25 illustrates the test image and its binary masks. Figure 3.25(b) shows that the gray level thresholding results in a mask consisting of a large number of misclassified ‘0’ pixels in homogeneous regions. By applying the procedure of the region correction depicted in Figures 3.22 and 3.23, two binary masks are generated as shown in Figure 3.25(c) and (d). Comparing the two masks, one can see the mask shown in (c) makes more pixels exposed than that shown in (d). Thus, the former is used for a more modest low-pass operation in an earlier stage than the latter. The low-pass operations in these stages will target the noise and artifacts in different categories of homogeneous regions. In the next section, the design of the stages of the low-pass filtering will be presented.

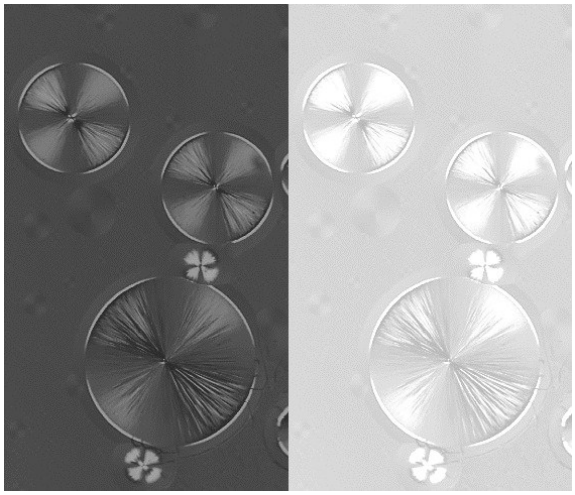

(a)

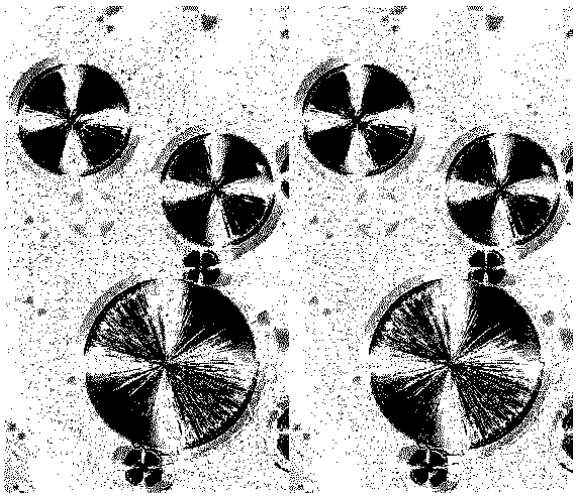

(b)

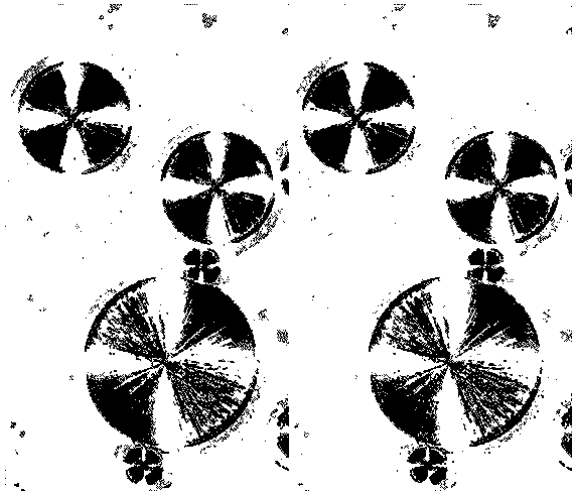

(c)

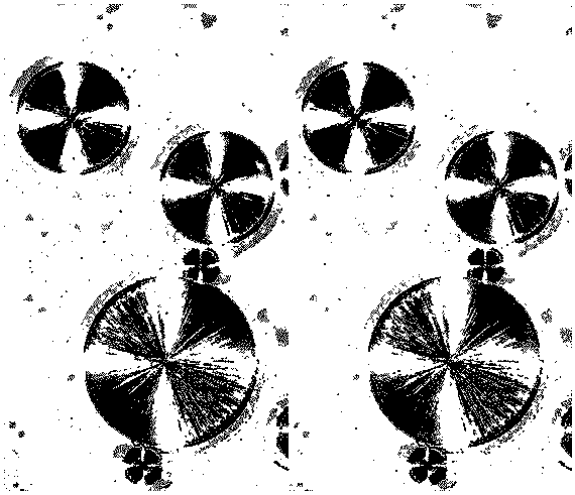

(d)

Figure 3.25 (a) Test image.
(b) Binary image I_{bw}' produced by the thresholding.
(c) Binary mask I_{bw1} produced by the procedure shown in Figure 3.22.
(d) Binary mask I_{bw2} produced by the procedure shown in Figure 3.23.

3.5 Low-pass filtering

The objective of this study is to get a good quality of image contrast enhancement by efficiently removing the noise and artifacts generated in the HE process while preserving the signal variations. The removal is done by means of a discriminative and progressive low-pass filtering.

To deal with different situations of noise and signal variations in the pre-filtered image, the low-pass operation will comprise multiple stages, in each of which a mask is applied to shield some areas in order to make the low-pass operation discriminative. In the first stage after the pre-filtering, the low-pass operation is to remove the gray level variations in homogeneous regions with a precaution as the pixels located closely to non-homogeneous regions are exposed for the filtering. In the following stage, the filtering operation should be made to erase the gray level variation more effectively in obvious-homogeneous regions. One can use the same type of filters in the first and second stages, in order to simplify the implementation. However, as the critical issues in the two stages can be very different in some applications, it would be reasonable also to employ different filters.

As mentioned previously, the pre-filtering operation is designed to remove the noise that has much higher frequency components than those of the signal. The remaining undesirable gray level variations created by an HE usually have medium and relatively low frequency components. The low-pass operation in each stage needs to be moderate, having some nature of pixel value preservation, while the strength of gray level smoothing is increasing by the successive stages.

A low-pass operation by a normal median filter is usually less affected by abnormally-looking pixel values likely resulting from noise contamination. Also, to give more chance of preserving original gray level variation, one can use a particular median filter, called bidirectional multistage median (BMM) [17], in which the center pixel value is made to have more priority in determining the result. The procedure of the filtering is shown in Figure 3.26. The operational window size can be 3x3 or larger, depending on the patterns of noises and artifacts. As this BMM filter has a property of a relatively good preservation of signal variation, it is chosen to be used in the first stage for a moderate filtering. If this filtering operation is performed more than once, the strength of smoothing will be progressed, which is needed for the noise removal in the homogeneous regions.

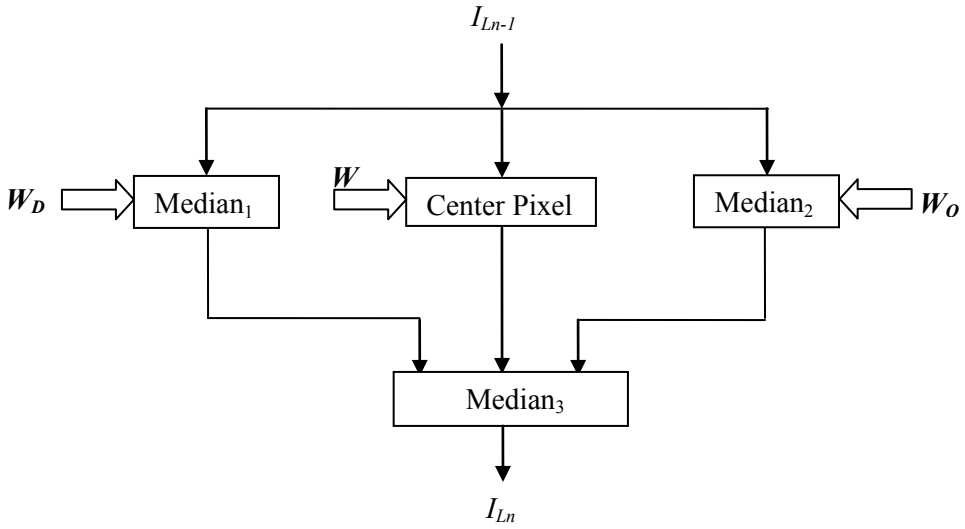

(a)

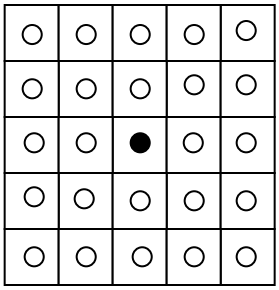

(b)

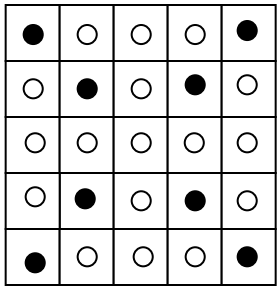

(c)

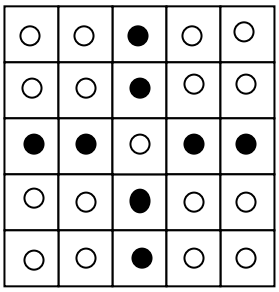

(d)

Figure 3.26 (a) Procedure of the bidirectional multi-stage median (BMM) filtering with three kernels, $\boldsymbol{W}$, $\boldsymbol{W_D}$ and $\boldsymbol{W_O}$. The median value of the pixels, of which the positions indicated by the solid dots, is taken as the result
(b) Center pixel kernel $\boldsymbol{W}$.
(c) Diagonal kernel $\boldsymbol{W_D}$.
(d) Orthogonal kernel $\boldsymbol{W_O}$.

Figure 3.27 shows the simulation results of the low-pass filtering processes. The input image (a) is produced by the Gaussian pre-filtering. The images (c) and (d) are generated by applying identical 5x5 BMM filters in the blocks of LP_1 and LP_2. The gray level variations in the homogeneous regions are reduced progressively with the stages of low-pass operations. The images shown in Figure 3.27(e) and (f) are obtained by using 5x5 Gaussian filters of $\sigma = 2$, instead of the BMM ones, in the stages of LP_1 and LP_2. Comparing the images shown in Figure 3.27(c) and (d) with those in (e) and (f), one can easily find that the BMM filtering better preserves image details in the regions of the third category, i.e., less-homogeneous regions. One example of such region is indicated by a dashed frame in Figure 3.27(a). The signal variations in such regions are well-preserved in the filtered images (c) and (d), whereas those in the filtered images shown in (e) and (f) are very much blurred.

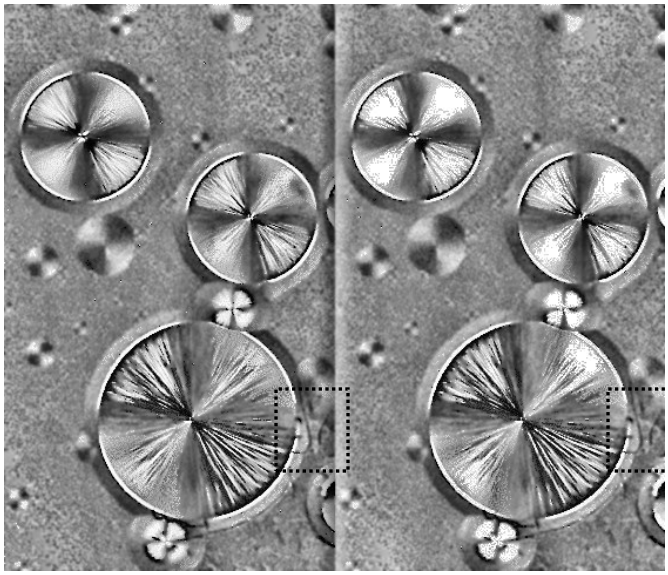

(a)

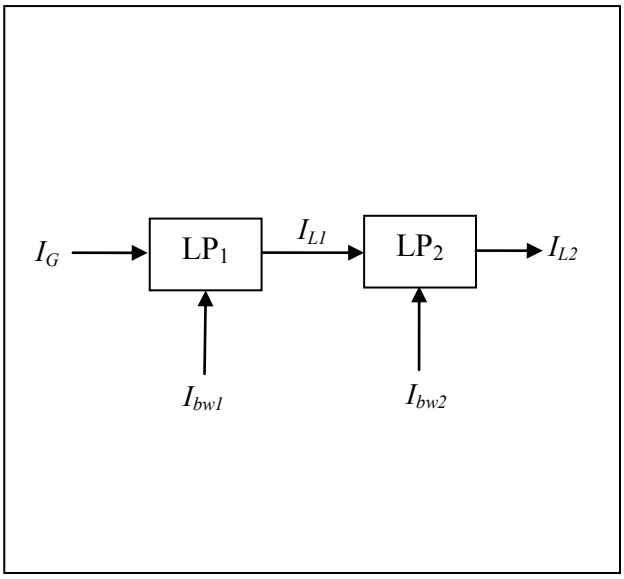

(b)

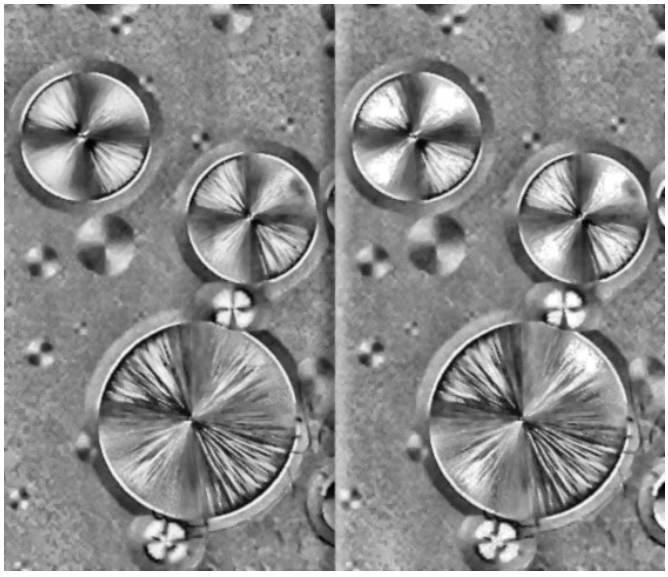

(c)

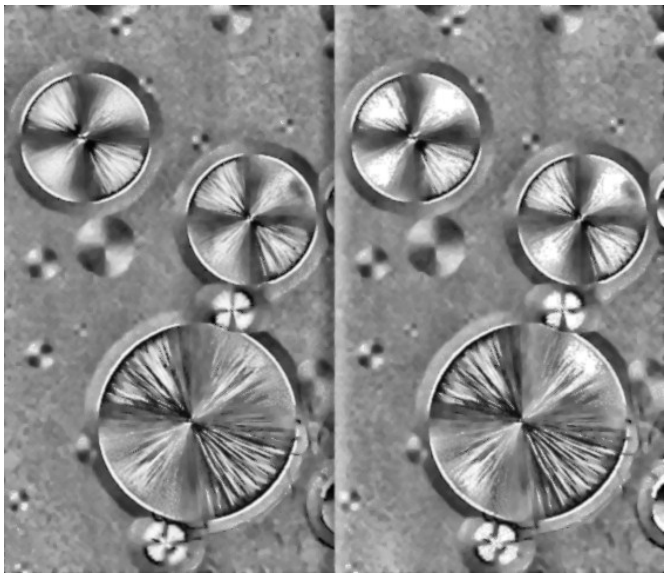

(d)

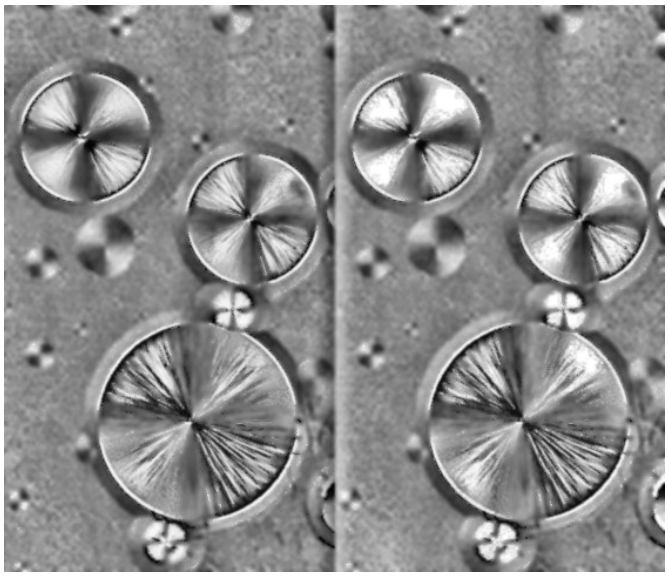

(e)

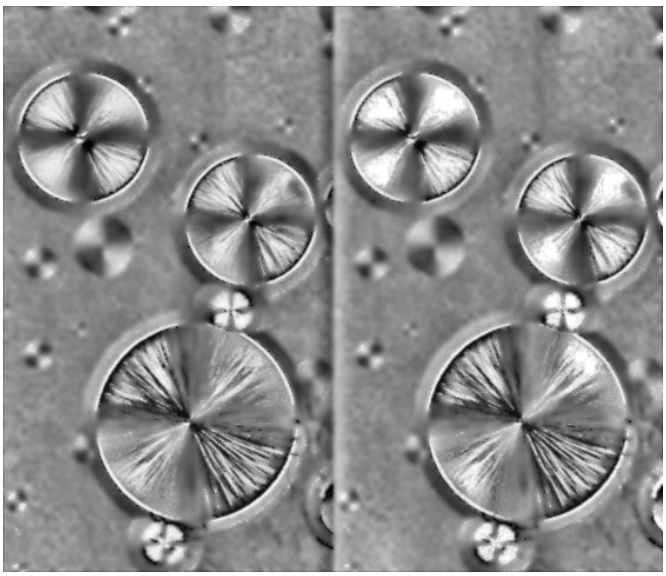

(f)

Figure 3.27 Results of the low-pass filtering processes using different filters.
(a) Pre-filtered image as the input $I_{G.}$
(b) Diagram of the discriminative low-pass filtering.
(c) Filtered image I_{L1} by one stage of BMM filtering.
(d) Filtered image I_{L2} by two stages of BMM filtering.
(e) Filtered image I_{L1} by one stage of Gaussian filtering with $\sigma = 2$.
(f) Filtered image I_{L2} by two stages of Gaussian filtering with $\sigma = 2$.

From the output results shown in Figure 3.27, one can conclude that the bidirectional multi-stage median filter can have a good preservation of signal variations, and a good smoothing strength if multiple stages are used. Therefore, it can be used effectively with the masks to remove the noise from the homogeneous regions without affecting the signal variations of non-homogeneous regions.

3.6 Summary

In this chapter, a method of contrast enhancement with noise and artifacts removal has been proposed. The challenge of this work is to design a discriminative and progressive low-pass filtering process to remove undesired gray level variations created by the HE process.

The noise and artifacts to be removed are found in the homogeneous regions, where there is no significant gray level variation before the histogram equalization. The strength of smoothing of the low-pass filtering should be strong in obvious-homogeneous regions and very weak in non-homogeneous regions. Different levels of low-pass filtering are implemented by successive stages of identical or non-identical filters. The gray level variation removal is increased stage by stage. Each low-pass operation is applied to the pixels selected by a binary mask. The pixels in obvious-homogeneous regions are exposed to all the low-pass operations and receive the strongest smoothing, while those located in the regions near non-homogeneous ones get a very moderate one.

The creation of the masks involves two steps of pixel classification. The first classification is done by means of a simple gray level thresholding in the histogram of the original image to classify coarsely the pixels of non-homogeneous regions and that of homogeneous regions. As the thresholding is too simplistic to do a fine classification, the thresholds are chosen to minimize the misclassification of the pixels truly belonging to non-homogeneous regions at the expense of increasing the misclassification of the pixels truly belonging to homogeneous regions. The second step, namely region correction, is to identify the misclassified pixels that should belong to homogeneous regions. It is done by detecting varieties of patterns formed by the misclassified pixels. Simple logic operations are used in the detection. Based on the result of the classification,

multiple binary masks are generated to shield the pixels of the non-homogeneous regions from different low-pass operations in multiple stages.

A low-σ Gaussian filter is used for the pre-filtering that is applied to the entire enhanced image to remove noise pitches. A moderate low-pass operation by a BMM filter is performed to all the pixels, except those in the non-homogeneous regions, to remove gray level variation with some precaution to avoid over-smoothing. A strong strength of smoothing is performed by multiple stages of BMM filters.

The computation in the low-pass stages and that for the classification is relatively simple. A short overall computation time should be expected. The proposed method has been applied to the test image and the results are promising. In the following chapter, the evaluation of its effectiveness will be described and the results will be presented.

Chapter 4

Performance evaluations and the simulation results

The objective of the work is to enhance the image contrast while minimizing the noise and artifacts. It is done by using the CLAHE method for the gray level variation enhancement and a novel discriminative low-pass filtering process. In this chapter, the proposed method is applied to several low-contrast images and the results are examined in a subjective and objective manner. Based on the results, the performance of the contrast enhancement combined with the filtering is evaluated. The results are compared with those produced by the iterated TMR filter reported in [23].

In the first part of this chapter, a subjective examination of the MATLAB simulation results is presented. Four images with different patterns are chosen and used in the simulation. The objective measurements are presented in the second part of the chapter.

4.1 Examination of the visual quality

In order to test the effectiveness of the discriminative noise removal in the proposed method, the images used in the simulation are from different categories, such as one from a medical imaging, a landscape, a microscopic sample and a poster. Figure 4.1 to 4.5 show the simulation results with those images. In each of those figures, the original input image, the image enhanced

by CLAHE and that obtained by the proposed method and that by the iterated TMR filtering method are presented. Three low-pass stages are used in the simulation of the proposed method. A Gaussian filter is used in the pre-filter stage and the 5x5 BMM filter in each of two other stages.

The simulation result with the image 'Chest X-ray' is shown in Figure 4.1. The original input has a very poor contrast and many small details are hardly seen. By means of the CLAHE enhancement with a clip limit of 0.04 and a tile size of 8x8, the contrast is significantly improved as shown in Figure 4.1(b). However, one can observe a significant increase of the noise by this enhancement in the image. By applying the proposed discriminative low-pass filtering, one can remove the noise and improve the image quality, which is shown in Figure 4.1(c). In the filtering process, the pre-filtering is done by a 5x5 Gaussian filter with $\sigma = 0.5$ followed by two stages of BMM filter. To generate the binary masks those are used in each of the BMM filtering stages, two sets of gray level values, (17, 22) and (136, 168) are used for thresholding and the algorithms shown in Figure 3.22 and 3.23 are used for region correction.

The iterated TMR filtering has also been applied to the CLAHE enhanced image shown in Figure 4.1(b) and the result is illustrated in Figure 4.1(d). The parameters used to get the results are found in Appendix I. Comparing the filtered image in Figure 4.1(c) and that in (d), one can see some significant differences demonstrating a much better noise removal in terms of preservation of image details performed by the proposed filtering process. In the image in Figure 4.1(c) processed by the proposed filtering, the details in the central spine are well preserved, so are those of blood vessels in the two sides of the spine, as well as the parts near the two armpits. These details in the image shown in Figure 4.1(d) are much more blurred.

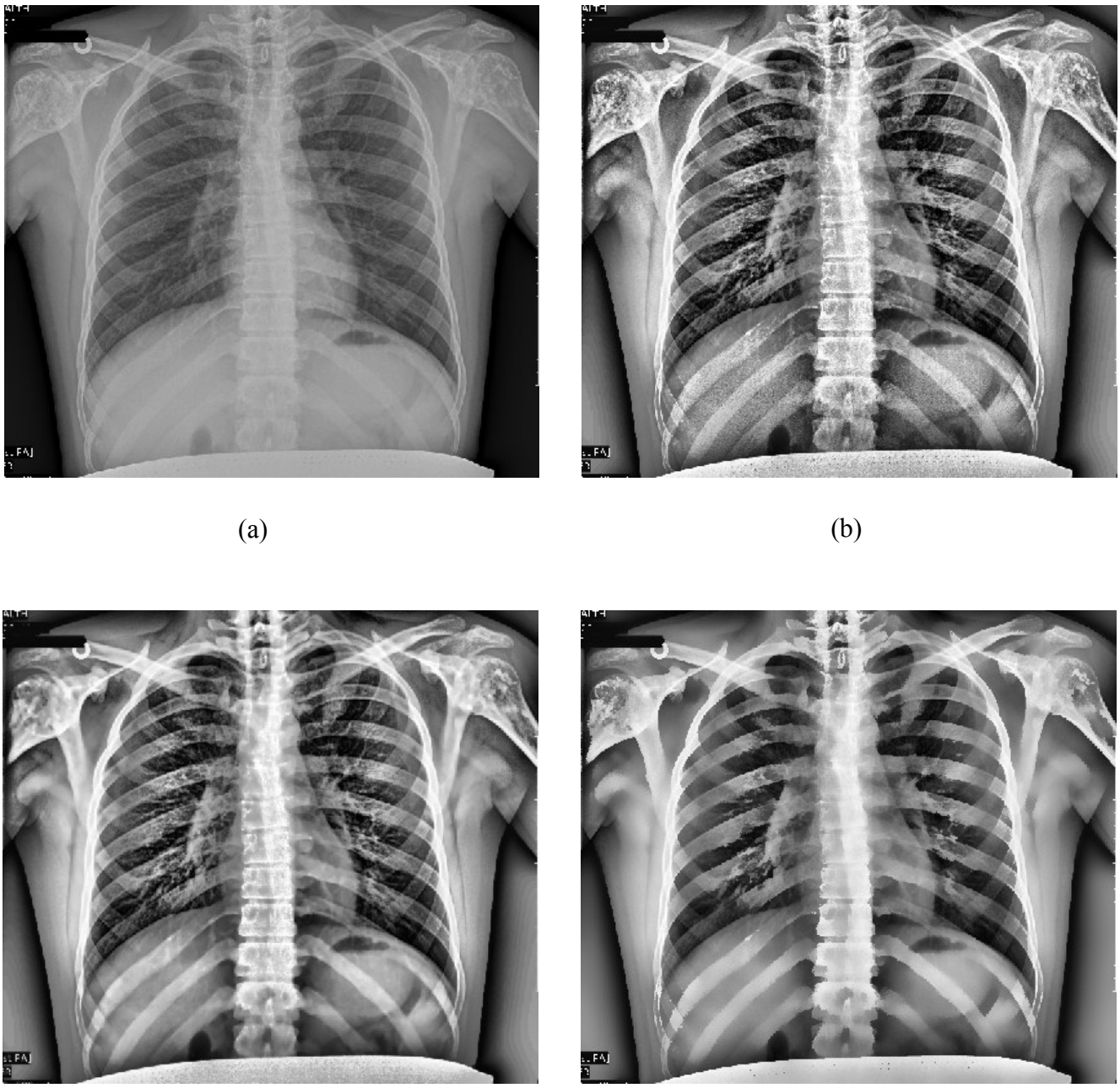

(a) (b)

(c) (d)

Figure 4.1 (a) Original image of 'Chest X-ray'.
(b) After the contrast enhancement by CLAHE.
(c) After the proposed low-pass filtering method.
(d) After the iterated TMR filtering.

The second image 'Window and Desk' used in the simulation, as shown in Figure 4.2(a), is a combination of interior scene and landscape. The contrast is very poor, but the image has very rich gray level variations in terms of patterns and frequencies. The result of the CLAHE enhancement is shown in Figure 4.2(b) and that after the proposed filtering in Figure 4.2(c). For the CLAHE enhancement, a clip limit of 0.03 and a tile size of 8x8 have been used. In the proposed filtering method, a 3x3 Gaussian filter with σ = 0.5 is used for the pre-filtering. To binarize the image, the threshold values of G_1 = 19 and G_2 = 34 are used and the algorithms shown in Figure 3.22 and 3.23 are employed to generate the two masks for the BMM filtering. Comparing the two images shown in Figure 4.2(b) and (c), one can see a better visual quality in the filtered one as the low-pass operations remove the noise created by the CLAHE process. To have a close observation of the image details, the lower half of each of the images in Figure 4.2(b), (c) and (d) are presented in Figure 4.3(a), (b) and (c), respectively. In the lower half of the CLAHE enhanced image shown in Figure 4.3(a), there is noise visible above the pens located in the left hand side and the bowl in the right side of the picture frame. Please note that these regions have a lot of gray level variations of image details. By using the proposed low-pass filtering, this noise is removed, as illustrated in Figure 4.3(b) while the image details in the regions are preserved. Comparing this filtered image with that processed by the TMR filtering shown in Figure 4.3(c), one can easily see the superior performance of the proposed one for the signal preservation. In Figure 4.3(b), the textures in the wall paper and those in the framed picture in the center are all clearly visible. They can hardly be seen in Figure 4.3(c).

(a) (b)

(c) (d)

Figure 4.2 (a) Original image 'Window and Desk' of a low-contrast landscape containing both under- exposed and over-exposed areas.
(b) After the contrast enhancement by CLAHE.
(c) After the proposed low-pass filtering method.
(d) After the iterated TMR filtering.

(a)

(b)

(c)

Figure 4.3 (a) Lower half of the 'Window and Desk' image after the CLAHE enhancement.
(b) After the proposed filtering method.
(c) After the iterated TMR filtering.

The third image 'Pollen Grain' used in the simulation shown in Figure 4.4(a) is taken from a microscopic sample of pollen grains which has a very low-contrast. It consists of many small objects with a lot of signal variations in each of it. By using the CLAHE method with a clip limit of 0.02 and a tile size of 8x8, its contrast is enhanced which is shown in Figure 4.4(b). The enhanced image has visible noises around the edges of each object. In the simulation of the proposed method, the pre-filtering is of a 3x3 Gaussian with $\sigma = 0.1$, thresholding of $(G_1, G_2) \equiv$ (81, 87) and (102, 105). The result is shown in Figure 4.4(c). After the proposed filtering, the noise around the objects is removed. Comparing this filtered image with that processed by the TMR filtering shown in Figure 4.4(d), it can be said that the image details are visibly preserved. In the framed region, for example, the gray level variations are well kept by the proposed filtering. They are flattened by the TMR filtering.

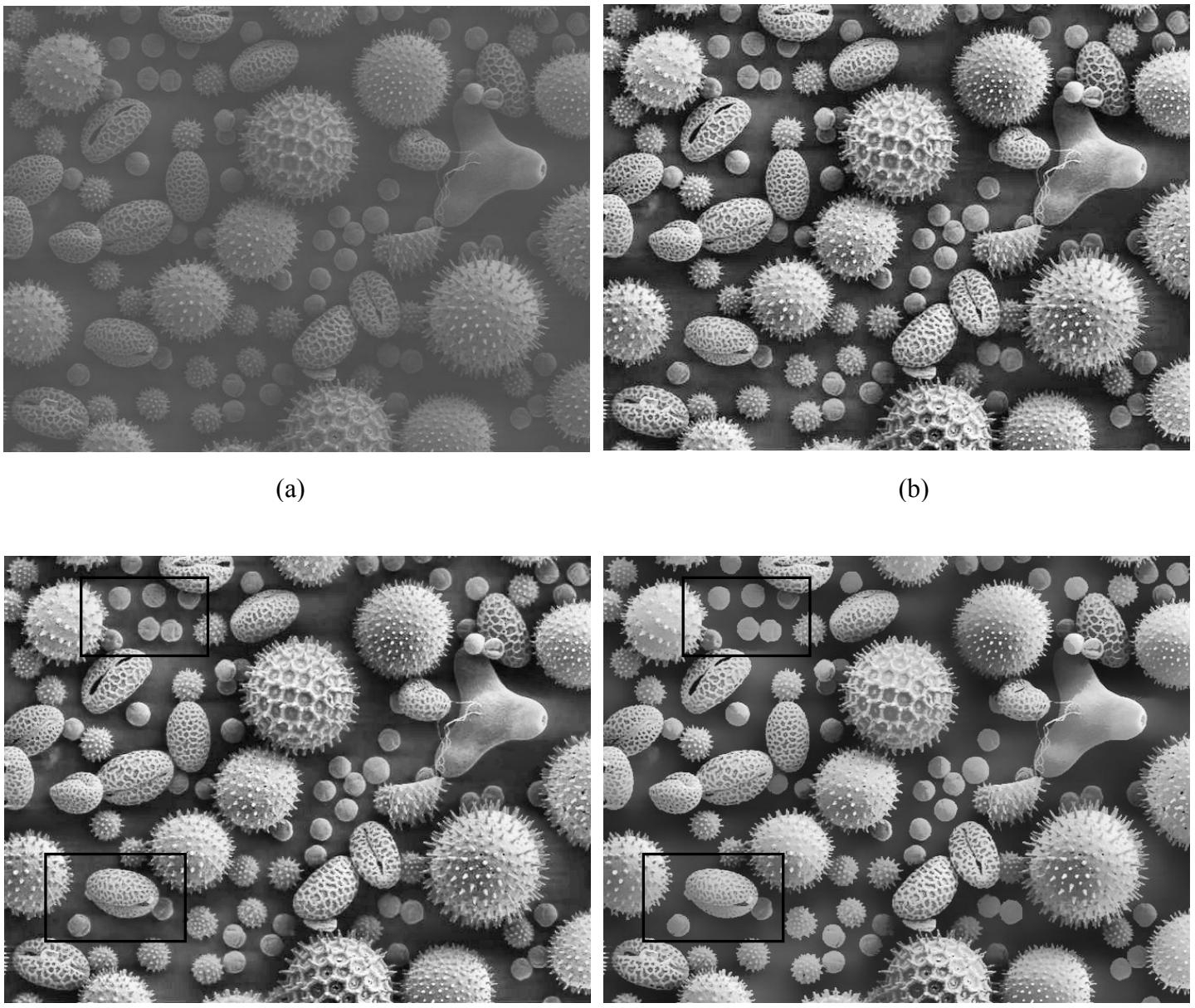

(a) (b)

(c) (d)

Figure 4.4 (a) Original image ‘Pollen Grain’ of a low-contrast microscopic image of pollen grains.
(b) After the contrast enhancement by CLAHE.
(c) After the proposed low-pass filtering method.
(d) After the iterated TMR filtering.

Figure 4.5(a) is a low-contrast poster image. It has been used in [23]. Its contrast is enhanced by the CLAHE method with the clip limit of 0.04 and the tile size of 8x8 as shown in Figure 4.5(b). In the simulation of the proposed filtering, Gaussian filter of 5x5 and $\sigma = 0.7$ is used for the pre-filtering followed by three stages of BMM filtering. The masks used in the first two stages are identical to those in the simulation with the other images. The last stage is to repeat that in the second stage for more smoothing in the homogeneous regions. In the image processed by the proposed filtering shown in Figure 4.5(c), the noise is significantly reduced while the contrast improved by the CLAHE maintained. However, the image produced by the TMR filtering, shown in Figure 4.5(d), is also based on the CLAHE-enhanced image, but the contrast is reduced again by the filtering.

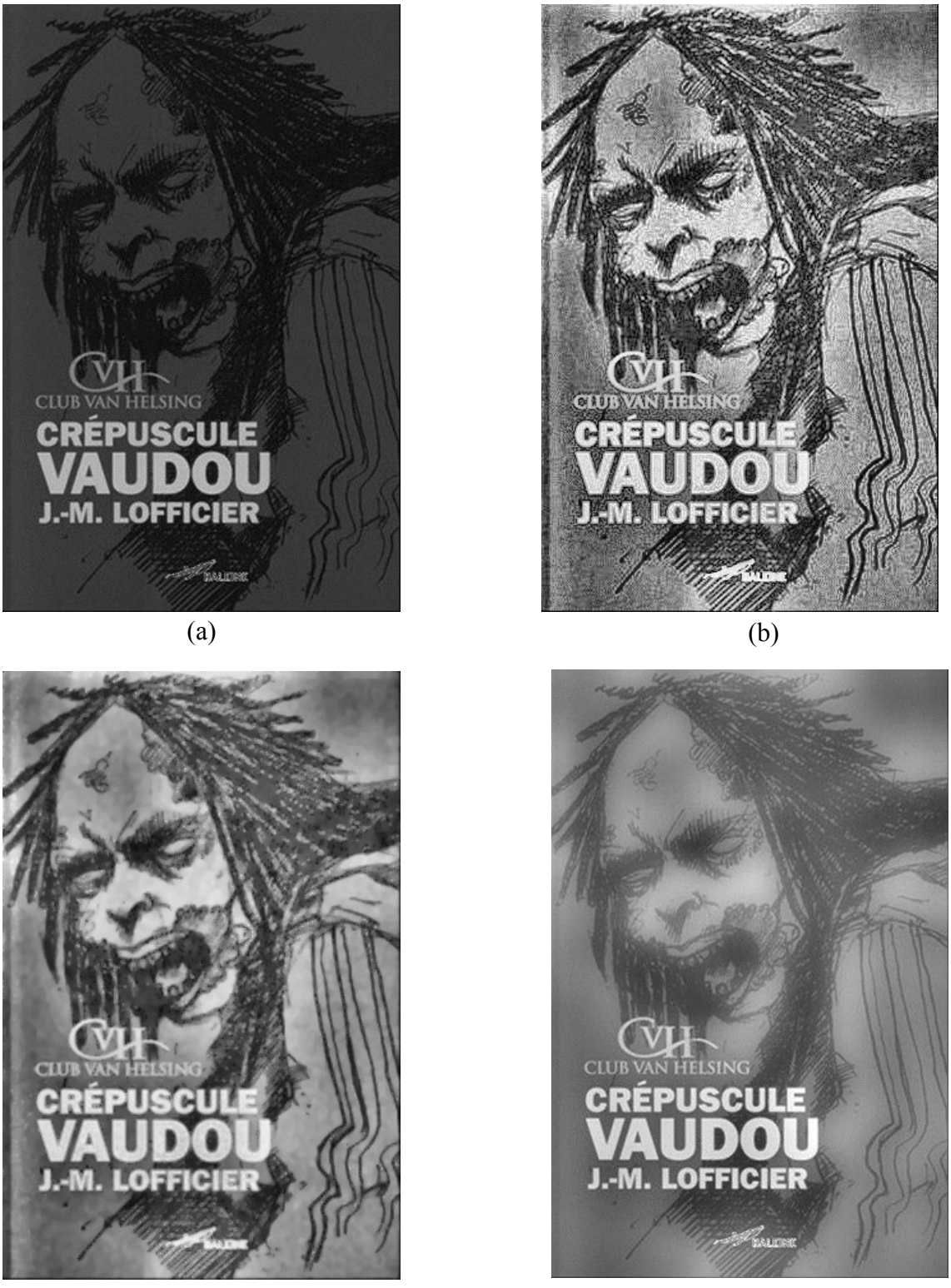

(a) (b)

(c) (d)

Figure 4.5 (a) Original image of a low-contrast poster.
(b) After the contrast enhancement by CLAHE.
(c) After the proposed low-pass filtering method.
(d) After the iterated TMR filtering.

From the above observation on the processed images and the comparison of the results with some relevant work, one can conclude that the proposed method yields a significant improvement in the HE-based contrast enhancement in terms of low noise and better signal preservation. In the next section, some objective measurements are presented to confirm the improvement.

4.2 Evaluation of signal-noise ratio and edge preservation

The quality of the contrast enhancement process can be measured by the amount of computation. It can be interpreted by the time required for the computation if the computing facility is given. The quality of the enhanced image is often evaluated by peak signal to noise ratio (PSNR). As the preservation of the signal variations in the filtering is a critical issue, Pratt's Figure of Merit (PFOM) is also used in the quality assessment of the edge maps generated from the images processed.

The computation of the proposed contrast enhancement with the filtering is implemented in MATLAB and the required computation time is calculated based on the elapsed time. This measurement of time is to indicate the volume of computation instead of processing speed. All the simulations are performed in the environment of intel Core 5i microprocessor @ 2.4GHz. For each input image, the elapsed time is measured and the average value of ten runs is taken as the computation time. The result is presented in Table 4.1. It also includes the computation time for the enhancement involving the TMR filtering for comparison. The data shown in this Table demonstrate that the proposed method results in shorter computation time, i.e., smaller volume of computation for the enhancement. In some cases the difference is very significant. For the

images of the same dimension, the computation time of the proposed method may vary, because the number of the pixels involved in different stages of the low-pass filtering varies. However, compared to that of the TMR filtering method, this variation of time is much less significant. It implies that the volume of computation of the proposed method is much less and more predictable, even with some variations than that of the iterated TMR filtering.

Table 4.1 Average elapsed time in second

Input image	Image dimension	Iterated TMR filtering based method	Proposed method
Chest X-ray	549x623	16.41	13.9
Window and Desk	800x854	48.9	10.84
Pollen Grain	512x672	25.2	9.56
Poster	476x311	8.78	8.15

The PSNR is most commonly used as a measure of the quality of an image. It is defined as

$$PSNR = \ 20.log_{10}\left(\frac{I_{max}}{\sqrt{MSE}}\right),$$

where I_{max} is the maximum possible pixel value of the image and *MSE* is the mean squared error of the enhanced image of m x n pixels, expressed as

$$MSE = \frac{1}{mn}\sum_{i=0}^{m-1}\sum_{j=0}^{n-1}[I(i,j) - I_e(i,j)]^2$$

with I and I_e being reference and enhanced images, respectively.

In this work, the visualized HDR images of the two images, namely ‘Window and Desk’ and ‘Pollen Grain’, are used as the reference ones. The PSNR values of the two images, enhanced by

the proposed method and the iterated TMR filtering method, are measured by CVIPtools provided in [7]. The results are presented in Table 4.2.

The performance of signal preservation can be objectively measured by Pratt's Figure of Merit (PFOM). It is calculated based on the comparison of the edge map I_I generated from the reference image and that of the image to be evaluated. Mathematically,

$$PFOM = \frac{1}{I_N} \sum_{i=1}^{I_F} \frac{1}{1 + \alpha d_i^{\,2}}$$

where:

I_N: the maximum of I_I and I_F.

I_I: the number of edge points in the edge map generated from the reference image .

I_F: the number of edge points found in the edge map to be evaluated.

α: a scaling constant used to adjust the penalty for offset edges, usually set to 1/9.

d_i: the distance of a found edge point to that in the reference edge map.

If the edge map to be evaluated is identical to the reference, the PFOM will be equal to 1, otherwise between 0 and 1. The PFOM values of the two images used earlier for measuring PSNR are obtained by using CVIPtools and also presented in Table 4.2. The edge map of each of the processed images and that of the corresponding visualized HDR image are generated by using Canny edge detector. The measurement confirms that the proposed method has a noticeably better capability of edge preservation while that of the noise removal is as good as that in [23]. This is achieved with much less computation requirement.

Table 4.2 PSNR and PFOM values of the two processed images

Input image	PSNR(dB)		PFOM	
	Iterated TMR filtering based method	Proposed method	Iterated TMR filtering based method	Proposed method
'Window and Desk'	15.697	15.758	0.9258	0.9536
'Pollen Grain'	12.641	12.5	0.9160	0.9507

4.3 Summary

In this chapter, the proposed method of low-noise contrast enhancement is evaluated by subjective observation and objective measurements. Simulation results are compared with a state of the art method.

The simulation results show that the proposed method is able to yield sufficient enhancement of contrast with effective removal of noise and artifacts. It also facilitates a very good preservation of signal variations. The better performances of the proposed method are also confirmed by the objective measurements.

Chapter 5

Conclusion

Contrast enhancement is one of the most commonly used operations in image pre-processing as an image acquisition or transmission may degrade signal gradients of images, and a sufficient gray level variation representing the image signal is essential for almost all the image processing procedures. Many methods have been proposed to enhance the image contrast. Most of them are based on histogram equalization. A simple procedure of HE makes the gray level variations enhanced indiscriminately, no matter that they are of signal or noise. It is thus a challenging task to enhance the signal gray level contrast and to remove the noise.

The work present in this thesis is about the development of an effective method of low-noise contrast enhancement. It uses CLAHE procedure to enhance the gray level variations and a low-pass filtering is proposed to remove the noise created by CLAHE. The emphasis in the development of the filtering process is to make the low-pass operations applied discriminatively in the image space in order to preserve the signal gray level variations of the image.

The proposed filtering process provides different levels of low-pass operations to suit different smoothing requirement in different regions in the image. It is done by progressive low-pass operations in successive filter stages. The first stage is made for a pre-filtering, and a weak smoothing operation is applied to all the pixels. In each of the other stages, the pixels to be processed are selected by a binary mask. Pixels in homogeneous regions, where a good strength of smoothing is needed, are exposed to multiple low-pass operations in the successive stages,

whereas those in less homogeneous regions will be open to one or two moderate smoothing and masked from further operations.

To generate the binary masks used in the proposed filtering process, the pixels of the image need to be classified. As the noise created by the HE process is more pronounced in homogeneous regions, it is reasonable to divide the pixels into different categories of regions according to the homogeneity of the pixel gray levels in the input image. There can be three categories of regions, such as obvious-homogeneous regions, obvious non-homogeneous regions and less homogeneous regions in the image. Hence, the pixels are classified into three groups corresponding to these three categories. The procedure of the classification consists of two steps. In the first step, by means of a simple gray level thresholding, the pixels are coarsely divided into two groups, homogeneous and non-homogeneous, represented by logic '1' and '0', respectively. The effort is made to minimize the risk of placing pixels located in non-homogeneous regions into the homogeneous pixel group. The second step, called the region correction, is to identify the misclassified pixels and correct their status. The identification is done by detecting patterns formed by misclassified pixels, which is implemented by simple logic operations.

Very simple low-pass filters are used in the filtering stages. A Gaussian filter with a low σ value can be used for the pre-filtering to remove high frequency pitches, and median-based filters in the successive stages.

The computational complexity of the contrast enhancement process, including CLAHE and the proposed discriminative filtering, is kept low. MATLAB simulation has been performed to evaluate the overall effectiveness of the process, its noise removal and signal preservation capabilities. The results demonstrate that the images processed by the proposed method have

superior quality in terms of subjective observation and objective measurements, compared to those reported in the literature.

There are several possibilities of future works related to this thesis that could increase the design flexibility and strengthen the performance of the proposed method. One such possibility is to perform extensive analysis and experimentation to decide optimal threshold values involving the classification procedure for different kinds of images. Another extension of this work could be tuning the low-pass filtering operation for removing the noises and artifacts created in the processes other than the HE.

References

[1] K. Zuiderveld, "Contrast Limited Adaptive Histogram Equalization," in *Graphics Gems IV*, San Diego, Academic Press Professional, 1994, pp. 474-485.

[2] D. Ballard and C. Brown, Computer Vision, Englewood Cliffs, NJ: Prentice-Hall, 1982.

[3] A. Rosenfeld and A. Kak, in *Digital Picture Processing*, vol. 2, Newyork, Academic Press, 1982.

[4] I.-Y. Jung and C.-S. Kim, "Image Enhancement using Sorted Histogram specification and POCs post-processing," in *IEEE International Conference on Image Processing*, 2007.

[5] S. Mann and R. Picard, "On Being 'undigital' With Digital Cameras: Extending Dynamic Range By Combining Differently Exposed Pictures," Perceptual Computing Section, Media Laboratory, Massachusetts Institue of Technology, 1995.

[6] S. M. Pizer, "Adaptive Histogram Equalization and Its Variations," in *Computer Vision Graphics and Image Processing*, 1987.

[7] S. E. Umbaugh, Computer Imaging: Digital Image Analysis and Processing, CRC Press, 2005.

[8] R. C. Gonzalez and R. E. Woods, Digital Image Processing, 2nd edition, Englewood Cliffs, NJ: Prentice Hall, 2002.

[9] L. Yaroslavsky, Digital Picture Processing: An Introduction, German: Springer-Verlag, 1985.

[10] J. Astola and P. Kuosmanen, Fundamentals of Non-linear Digital Filtering, New York: CRC Press LLC, 1997.

[11] Y. Gal, A. J. Mehnert, A. P. Bradley, K. McMahon, D. Kennedy and S. Crozier, "Denoising of Dynamic Contrast-Enhanced MR Images Using Dynamic Non-Local Means," *IEEE Transactions on Medical Imaging,* vol. 29, no. 2, pp. 302-310, 2010.

[12] A. Nieminen, P. Heinonen and Y. Neuvo, "A New Class of Detail-Preserving Filters for Image Processing," *IEEE Transactions on Pattern Analysis and Machine Intelligence,* Vols. PAMI-9, no. 1, pp. 74-90, 1987.

[13] J. Astola, P. Heinonen and Y. Neuvo, "Linear Median Hybrid Filters," *IEEE Transactions on Circuits and Systems,* vol. 36, no. 11, pp. 1430-1438, 1989.

[14] J.-Y. Kim, L.-S. Kim and S.-H. Hwang, "An Advanced Contrast Enhancement Using Partially Overlapped Sub-block Histogram Equalization," *IEEE Transactions on Circuits and Systems for Video Technology,* vol. 11, no. 4, pp. 475-484, 2001.

[15] T. K. Kim, J. K. Paik and B. S. Kang, "Contrast Enhancement System Using Spatially Adaptive Histogram Equalization With Temporal Filtering," *IEEE Transactions on Consumer Electronics,* vol. 44, no. 1, pp. 82-87, 1998.

[16] B. Justusson, Median Filtering: Statistical Properties, Topics in Applied Physics, Two-Dimensional Digital Signal Processing II, vol. 43, Berlin: Springer-Verlag, 1981, pp. 161-196.

[17] G. Arce and F. R.E., "Detail-preserving Ranked-order Based Filters For Image Processing," *IEEE Transactions on Acoustics, Speech and Signal Processing,* vol. 37, no. 1, pp. 83-98, 1989.

[18] A. C. Bovik, S. J. Aggarwal, N. H. Kim and K. R. Diller, "Quantitative Area Determination of Computer Image Analysis," in *Image Analysis in Biology*, Florida, CRC press, 1991, pp. 35-38.

[19] D. Brownrigg, "The Weighted Median Filter," *Communication of the ACM,* vol. 27, no. 8, pp. 807-818, 1984.

[20] A. Buades, B. Coll and J. Morel, "A Review of Image Denoising Algorithms, with A New One," *Multiscale Modeling and Simulation,* vol. 4, no. 2, pp. 490-530, 2005.

[21] S. Cvetkovic, J. Schirris and P. de With, "Nonlinear Locally-adaptive Video contrast Enhancement Algorithm without Artifacts," *IEEE Transactions on Consumer Electronics,* vol. 54, no. 1, pp. 1-9, 2008.

[22] P. Perona and J. Malik, "Scale-space and Edge Detection Using Anisotropic Diffusion," *IEEE Transactions on Pattern Analysis and Machine Intelligence,* vol. 12, no. 7, pp. 629-639, 1990.

[23] J. Rabin, J. Delon and Y. Gousseau, "Removing Artefacts from Color and Contrast modifications," *IEEE Transaction on Image Processing,* vol. 20, no. 11, pp. 3073-3085, 2011.

[24] P. Sahoo, S. Soltani and A. Wong, "A Survey of Thresholding Techniques," *Computer Vision, Graphics, and Image Processing,* vol. 41, no. 2, pp. 233-260, 1988.

[25] J. Stark, "Adaptive Image Contrast Enhancement using Generalizations of Histogram Equalization," *IEEE Transactions on Image Processing,* vol. 9, no. 5, pp. 889-896, 2000.

[26] C. Tomasi and R. Manduchi, "Bilateral Filtering for Gray and Color Images," in *International Conference on Computer Vision*, 1998.

[27] Y.-T. Kim, "Contrast Enhancement Using Brightness Preserving Bi-histogram Equalization," *IEEE Transactions on Consumer Electronics,* vol. 43, no. 1, pp. 1-8, 1997.

[28] S.-D. Chen and A. Ramli, "Minimum Mean Brightness Error Bi-Histogram Equalization in Contrast Enhancement," *IEEE Transactions on Consumer Electronics,* vol. 49, no. 4, pp. 1310-1319, 2003.

[29] H. Demirel, C. Ozcinar and G. Anbarjafari, "Satellite Image Contrast Enhancement Using Wavelet Transform and Singular Value Decomposition," *IEEE Geoscience and Remote Sensing Letter,* vol. 7, no. 2, pp. 333-337, 2010.

[30] J.-L Starck, F. Murtagh; E. J. Candes and D.L. Donoho, "Gray and Color Image Contrast Enhancement by the Curvelet Transform," *IEEE Transactions on Image Processing,* vol.12, no. 6, pp. 706-717, 2003.

[31] F. Lamberti, B. Montrucchio and A. Sanna, "CMBFHE: A Novel Contrast Enhancement Technique Based on Cascaded Multistep Binomial Filtering Histogram Equalization," *IEEE Transactions on Consumer Electronics,* vol.52, no. 3, pp. 966-974, 2006.

[32] Hyung-Seung Lee, Rae-Hong Park and Sunghee Kim, "Adaptive Video Enhancement Using Neural Network," *IEEE Transactions on Consumer Electronics,* vol.55, no. 3, pp. 1637-1644, 2009.

[33] Alan C. Bovic, The Essential Guide to Image Processing, 2nd edition, Academic Press, 2009.

[34] Photo albums, http: //www.hdrsoft.com/index.html.

[35] *Easy HDR Pro tutorial*, http://www.easyhdr.com/tutorial.php?sub=2.

[36] Maria Petrou, Costas Petrou, Image Processing: The Fundamentals, 2nd edition, Wiley, 2010.

[37] William K. Pratt, Digital Image Processing, 4th edition,Wiley-Interscience,1991.

Appendix I

Values of the parameters used in the simulation of TMR filtering [23]

Image	No. of iterations	Radius of disk, W	Intensity domain standard deviation, σ
Chest X-ray	3	5	0.07
Window and Desk	3	10	0.04
Pollen Grain	3	10	0.05
Poster	3	10	10